ELSEVIER

Synthesis, structure and reactivity of homobimetallic Rh(I) and Ir(I) complexes of *s*- and *as*-indacene-diide

Alberto Ceccon [a,*], Annalisa Bisello [a], Laura Crociani [a], Alessandro Gambaro [a],
Paolo Ganis [a], Francesco Manoli [b], Saverio Santi [a], Alfonso Venzo [b]

[a] *Department of Physical Chemistry, University of Padova, via Loredan 2, I-35131 Padua, Italy*
[b] *CNR, Centro di Studi sugli Stati Molecolari Radicalici ed Eccitati, via Loredan 2, I-35131 Padua, Italy*

Abstract

The Rh(COD) and Ir(COD) homobimetallic complexes of *s*-indacene-diide, 2,6-dimethyl-*s*-indacene-diide, *as*-indacene-diide, and 2,7-dimethyl-*as*-indacene-diide have been synthesized from the di-lithium salts of the dianions and metal dimers $[M(\mu\text{-Cl})L_2]_2$ (M = Rh, Ir; L_2 = COD, NBD, (ethylene)$_2$, (CO)$_2$) as mixtures of *syn* and *anti* isomers. The *syn/anti* ratio depends on the nature of the ancillary ligands at the metal and on the *s* or *as* geometry of the bridging ligand. In the reaction of the 2,7-dimethyl-*as*-indacene-diide-$[M(COD)]_2$ species with CO, the higher reactivity of the *syn* isomers has been justified on the basis of a greater instability of the ground state due to steric interactions between the COD groups. Bis-η^1 metal-bonded intermediates have been identified in the carbonylation of iridium derivatives; on the other hand, the formation of the bis-η^5 mixed complexes *syn* and *anti*-{2,7-dimethyl-*as*-indacene-diide-[Rh(COD)][Rh(CO)$_2$]} and their reactivity strongly support the existence of metal–metal interaction in the rhodium derivatives. © 2000 Elsevier Science S.A. All rights reserved.

Keywords: Indacene-diide complexes; Rhodium complexes; Iridium complexes; *Syn/anti* isomers; Cooperative effects

1. Introduction

The growing interest in the polymetallic complexes of organic ligands arises from the possible existence of some kind of interaction between the metal centers so that the properties of one site can be finely tuned by both the presence and the intrinsic properties of a second inorganic group [1]. In particular, the interaction between the metal centers is expected to influence their structural, spectroscopic, chemical (e.g. the reactivity both in stoichiometric and catalytic processes) and physical properties (e.g. magnetism, optical linearity, etc.) when compared with the behavior of the analogous monometallic compounds.

The possibility of investigating these *cooperative effects* is clearly correlated with the ability to solve the problem of anchoring two (or more) metals in close proximity with a certain geometry through an appropriate *bridging ligand* having several coordination sites

available. In other words, one has to project the right *spacer* able to route the interaction from one active center to the other:

$$L_nM \!\!-\!\!\boxed{\text{SPACER}}\!\!-\!\!M'L'_{n'}$$

The cooperative effects may arise (i) from a strong through-bond interaction transmitted by a suitable bridging ligand; or (ii) from a direct metal-to-metal bond interaction depending on the electronic and steric properties of the ligand and on the relative geometric dispositions of the metals themselves.

Many classes of multi-site bridging ligands have been investigated thoroughly. Among them we cite the bis-cyclopentadienyl derivatives in which the two five-membered rings are bonded directly (*fulvalene* systems) or connected through a saturated or unsaturated chain [2]. However, in this class of compounds, the orientation and the distance between the metals is not certain due to the noticeable flexibility of the ligand, so that the chemical and physical behavior is often puzzling and cannot be justified unambiguously. Conversely, *ortho-*

* Corresponding author. Fax: + 39-049-8275135.
E-mail address: a.ceccon@chfi.unipd.it (A. Ceccon)

condensed bicyclic ten π-electron ligands, such as the neutral naphthalene, the monoanionic indenide and the bis-anionic pentalene-diide species can furnish (i) a rigid skeleton and (ii) a more delocalized ten π-electron system ensuring a fixed geometry and a suitable transmission of the electronic interactions between the metals. In the bimetallic complexes of these bridging ligands, a transoid (*anti*) and a cisoid (*syn*) disposition of the two metal groups are possible. In fact, in the case of pentalene-diide, only *anti* bimetallic complexes have been reported [3], while for the naphthalene [4] and indenide [5], bridging ligands *syn* and *anti* compounds have been obtained if the appropriate synthetic pathway is adopted.

In this paper we shall describe the investigation we have performed on some bimetallic complexes having the indacene-diide dianion as the bridging ligand. Owing to the high delocalizability of its 14 π-electron system, both *s* ands *as* isomers of this condensed aromatic spacer have been identified as suitable bridging ligands in view of strong electronic interactions between the coordinated metal centers, which may result in interesting chemical and physical properties [6]. We note, however, that the electronic structures of the two isomeric dianions have been determined recently by EHMO calculations [7]. Differences in the HOMO–LUMO gap in the two ligands have been reported so that, at least in principle, different reactivity of the two isomers could be expected.

A generally reported synthetic procedure of some bimetallic indacenyl complexes consists of the reaction of indacene-diide dilithium salts with mononuclear or dinuclear metal reagents. However, the stereochemical control of the reaction is a vexing problem. Groups such as MCp or MCp* (Cp = C_5H_5, Cp* = C_5Me_5; M = Fe, Co, Ni) coordinate exclusively *anti* [8]; conversely, mixtures of *syn* and *anti* isomers have been obtained for metal carbonyls complexes of manganese [9]. Finally, recent results by O'Hare and co-workers [10] on cobalt and iron complexes obtained by the reaction of the neutral 1,3,5,7-tetra-*t*-butyl-indacene with dinuclear reagents have shown the presence of the *syn* isomer only. These results seem to indicate that mononuclear metal reagents favor the formation of *anti* products, whereas binuclear reagents would favor the *syn* products. However, it should be noted that a correct comparison of the results is rather difficult because the reaction conditions differ greatly. Recently, we have prepared some Rh(I) and Ir(I) monometallic indacenyl complexes by quenching the lithium or potassium salts of *s*- and *as*-hydroindacenide ligands with the appropriate metal dimer. From these species, homobimetallic indacenyl complexes can be obtained by further deprotonation and reaction with the same metal dimers [11]. Here, we shall discuss the results obtained by the single-step synthesis of homo-bimetallic inda-

cenyl complexes by reaction of some *s*- and *as*-indacene-diides with metalating dimers of the type $[M-(\mu-Cl)L_2]_2$ (M = Rh, Ir), where L_2 represents one bidentate ligand (COD, NBD) or two monodentate ligands, viz., (ethylene)$_2$, (CO)$_2$.
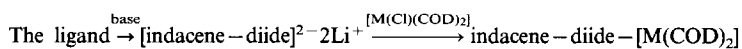
2. Results and discussion

In order to tackle this investigation correctly, strictly similar conditions for the bis-metalation reaction were adopted: indacene-diide dilithium salts were generated quantitatively from the corresponding hydrocarbons by using two equivalents of *t*-butyl-lithium as the deprotonating reagent in carefully dried and deoxygenated THF. The ionization was performed in the − 20 to − 30°C temperature range, and the salt was treated with two equivalents of dinuclear rhodium and iridium reagents at − 30°C. The solvent was pumped off at low temperature and the crude reaction mixture analyzed for the products by ^{1}H-NMR. The efficiency of this preparative pathway is quite good, and as an example, the yields obtained with COD as the ancillary ligand at the metal are summarized in Table 1.
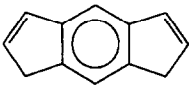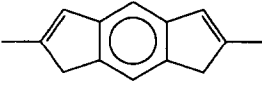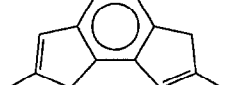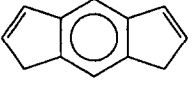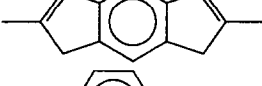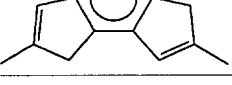
The almost quantitative yields of homobimetallic rhodium complexes observed both for *s* and *as* ligands strongly indicate that the double deprotonation of the starting neutral ligand is complete, and that the metalation reaction is rapid in comparison with side reactions (e.g. reaction of the dianion with other proton donors, electron transfer reactions, etc.). In the case of iridium species, the conversion and the yields of bimetallic complexes are somewhat lower. This difference could be accounted for by considering the different reactivity exhibited by the rhodium and iridium dimers [11]. If the dianions are consumed rapidly by the highly reactive dinuclear species [Rh(μ-Cl)(COD)]$_2$ to give the dimetalated complex, the yield of monometallic compounds appears to be quite low, whereas with the less reactive metalating reagent [Ir(μ-Cl)(COD)]$_2$, substantial amounts of monometallic hydroindacenide–Ir(COD) are produced as a results of rapid mono-protonation of the dianion. An alternative, but less convincing, explanation would be to attribute the formation of monometallic compounds to a lower stability of the di-iridium complexes of the indacenyl ligand in comparison with that of the di-rhodium complexes: they would suffer loss of one Ir(COD) unit and protonation to monometallic species.

2.1. The syn/anti ratios in homobimetallic indacene-diide complexes

The relative yields of the *syn* and *anti* bimetallic isomers in the one-step bis-metalation reaction are summarized in Table 2. We observe that (i) the *syn* isomer

Table 1

Organometallic product yields in the reaction of some s- and as-indacene-diides with $[M(\mu\text{-Cl})(COD)]_2$ [a]

The ligand $\xrightarrow{\text{base}}$ [indacene $-$ diide]$^{2-}$ 2Li$^+$ $\xrightarrow{[M(Cl)(COD)_2]}$ indacene $-$ diide $-$ [M(COD)$_2$]

Ligand	M	Conversion (%)	Relative yields (%)	
			Bimetallic complex [b]	Monometallic complex
[c]	Rh	80–90	>99	<1
	Rh	80–90	>99	<1
	Rh	80–90	>99	<1
	Ir	45	50	50
	Ir	65	70	30
	Ir	50	>99	<1

[a] Base, t-BuLi, 2.5 equivalents; solvent, THF; T 243 K.
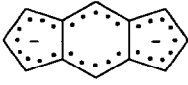
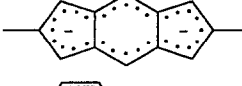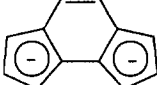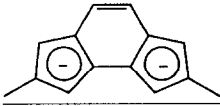[b] Mixture of syn and anti isomers, see text.

[c] As 50:50 mixture of 1,5- and 1,7-dihydro isomers, see text.

is favored when olefins are the ancillary ligands. The chelating olefins COD and NBD, for example, afford a great excess (90–82%, respectively) of the syn isomer with s-indacene-diide as a spacer; (ii) the ethylene as ancillary ligand induces a lower stereochemical preference; (iii) CO greatly favors the anti dispositions of the metal groups, the anti isomer being almost the unique product in the case of s-indacene-diide; (iv) in general, with the asymmetric indacene-diide as the bridging ligand, the syn/anti ratio is lower than that found for the symmetric ligand.

The explanation of these results is rather puzzling. A deeper insight into the problem may be provided by considering the structures of the two reagents involved in the metalation reaction, i.e. the di-lithium salt of s- and as-indacene-diide and the metal dimers. There is little information about the structure in solution of the salt; its structure is probably similar to that of $Li_2[1,3,5,7\text{-tetra-}t\text{-butyl-}s\text{-indacene-diide}]$ which has been reported recently [10c], where the two lithium cations (which coordinate to two THF molecules each) reside on opposite sides of the indacene-diide plane. This anti arrangement has been ascribed to electrostatic repulsions between the two lithium cations even though steric effects cannot be neglected on account of the

bulky $[Li(THF)_2]^+$ groups. An anti distribution of the two $[Li(TMEDA)_2]^+$ units has been found also in the solid-state structure of the silylated indacenyl species $Li_2[(\mu\text{-}Me_2Si)_2(C_5H_3)_2]$ [12]. The large $[Li(TMEDA)_2]^+$

Table 2

The effect of the ancillary ligand, L, on the syn/anti ratio in the one-step synthesis [a] of homobimetallic indacene-diide-$[RhL_2]_2$ complexes

	L$_2$			
	COD	NBD	(Ethylene)$_2$	(CO)$_2$
	9:1	4.5:1	1.5:1	1:19
	7:1	–	–	1:7
	3:1	3:1	2:1	1:5
	2:1	4.5:1	2:1	1:1.5

[a] For the experimental conditions, see footnote (a) of Table 1.
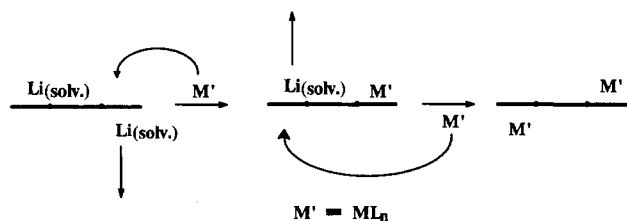
Scheme 1. The mechanism of *anti* isomer formation by a two-step metalation reaction.
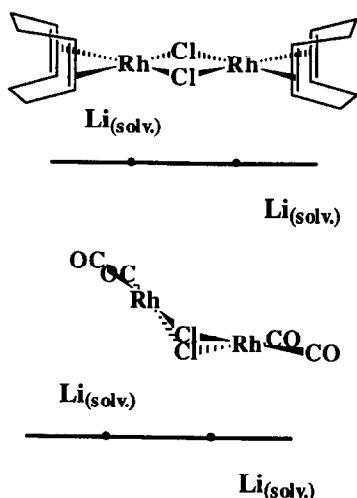
Scheme 2. The mechanism of the one-step bis-metalation with planar (upper part) and bent (lower part) metal dimers.

fragments seem also, in this case, to favor an *anti* arrangement for steric reasons.

A monomeric (or oligomeric) *anti* disposition of the two lithium ions, probably coordinated to THF molecules, in the ion pairs of the indacene-diide dianion should favor the formation of the *anti* bimetallic isomer by a two-step mechanism similar to that shown in the Scheme 1.

However, this is *not* in accordance with the majority of the results of Table 2, where a large preponderance of the *syn* isomer is reported, especially in those runs where the bidentate ancillary ligands COD and NBD have been used.

On the other hand, the structures of the metal dimers, $[M(\mu\text{-Cl})L_2]_2$, have been investigated since the 1960s, both in solution and in the solid state [13]. The rhodium derivatives show different characteristics depending on the nature of L. Thus, while the two rhodium and the two chlorine atoms lie on a plane with the olefin bonds perpendicular when L_2 is COD, the dimers with $L_2 = (CO)_2$ and $(\text{ethylene})_2$ show a bent geometry with the two $[RhCl(CO)_2]$ and $[RhCl(\text{ethylene})_2]$ planes intersecting at angles of 124 and 116°, respectively. As a consequence, the distance between the two rhodium atoms is longer in $[Rh(\mu\text{-Cl})(COD)]_2$ (3.50 Å) than in $[Rh(\mu\text{-Cl})(CO)_2]_2$ (3.12 Å).

The planar or bent structure of the dimer cores may play an important role in determining the geometry of the bimetallic indacenyl complex. To justify the results of Table 2, we suggest that planar dimers favor a concerted bis-metallation pathway shown in the upper part of Scheme 2, in which the two rhodium centers interact simultaneously at the same face of the bridging ligand to generate the *syn* isomer. Conversely, a bent structure of the dimer would disfavor the concerted one-step process if the approach to the indacene-diide is similar to that depicted in the lower part Scheme 2, and a two-step mechanism would become competitive especially with CO ligands.

In this hypothesis, the simultaneous attack of both the $[Rh(\mu\text{-Cl})(COD)]$ units at the Cp sites in the concerted path are expected to suffer in the transition state from noticeable steric effects. Thus, the lower *syn/anti* ratio observed for the *as*-indacene-diide isomer with respect to the *s*-indacene-diide can be attributed to steric effects, which should be of greater importance as the distance between the centroids of the Cp rings changes from ca. 5 Å in the *s* isomer to ca. 4 Å in the *as* derivative.

The results obtained in different laboratories seem to support the hypothesis of two competitive pathways. In fact, reaction with dinuclear reagents such as $Fe_2(CO)_9$ or $Co_2(CO)_8$ affords the *syn* bimetallic complex as the sole product [10], while *anti* bimetallic complexes were obtained when the metalation was carried out by large mononuclear metal fragments such as Cp^*M (M = Re and Ru) [8].

On the basis of these observations, it would be possible to suggest a modified interpretation of the isomeric ratios of Table 2. In THF, a strong coordinating solvent, the metal dimers may equilibrate with their monomers, the position of the equilibrium probably depending on the nature of the ancillary ligands. Thus, for COD and NBD dimers, the predominant path is that involving the concerted attack by the undissociated dimer, the *anti* isomer being formed through a two-step path by the monomer. From this point of view, the results obtained with $[Rh(\mu\text{-Cl})(CO)_2]_2$ as reagent suggest an increased dissociation of the dimer in solution, probably by a larger THF solvation of the monomer induced by the electronic effect of the CO.

In conclusion, whatever the cause for the different isomer ratios, it has been ascertained that by changing the nature of the ancillary ligands one can obtain mixtures with a large preference for the *syn* (with COD or NBD) or *anti* (with CO) derivative. On a preparative scale, since the substitution of the ancillary ligands is an easy reaction that does not change the stereochemistry of the complex, it would be rather feasible to obtain couples of *syn/anti* complexed isomers by ligand exchange with the appropriate reagent [5].

anti-**Rh₂**

syn-**Rh₂**

Fig. 1. ORTEP view of the structure of *anti*-{2,7-dimethyl-*as*-indacene-diide}-[Rh(COD)]₂} (*anti*-Rh₂), and *syn*-{2,7-dimethyl-*as*-indacene-diide}-[Rh(COD)]₂} (*anti*-Rh₂). The pertinent hydrogen atoms are evidenced.
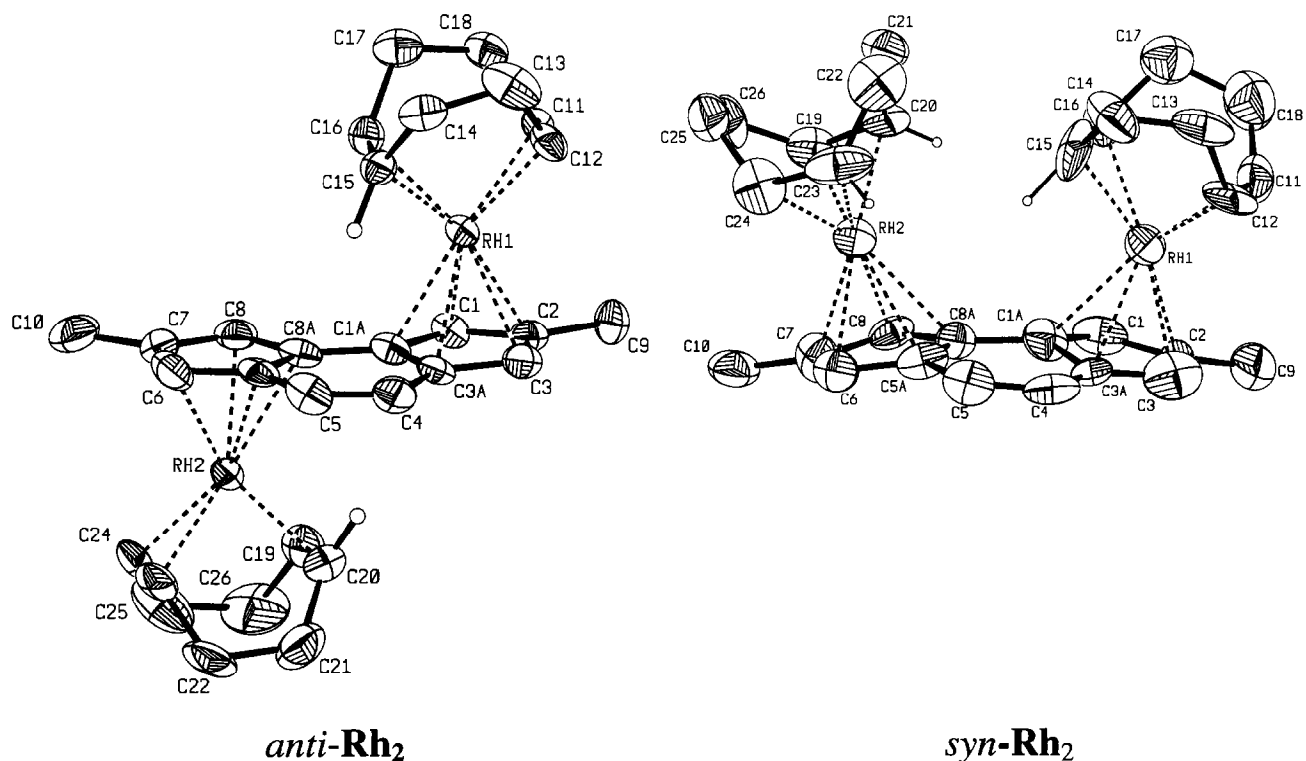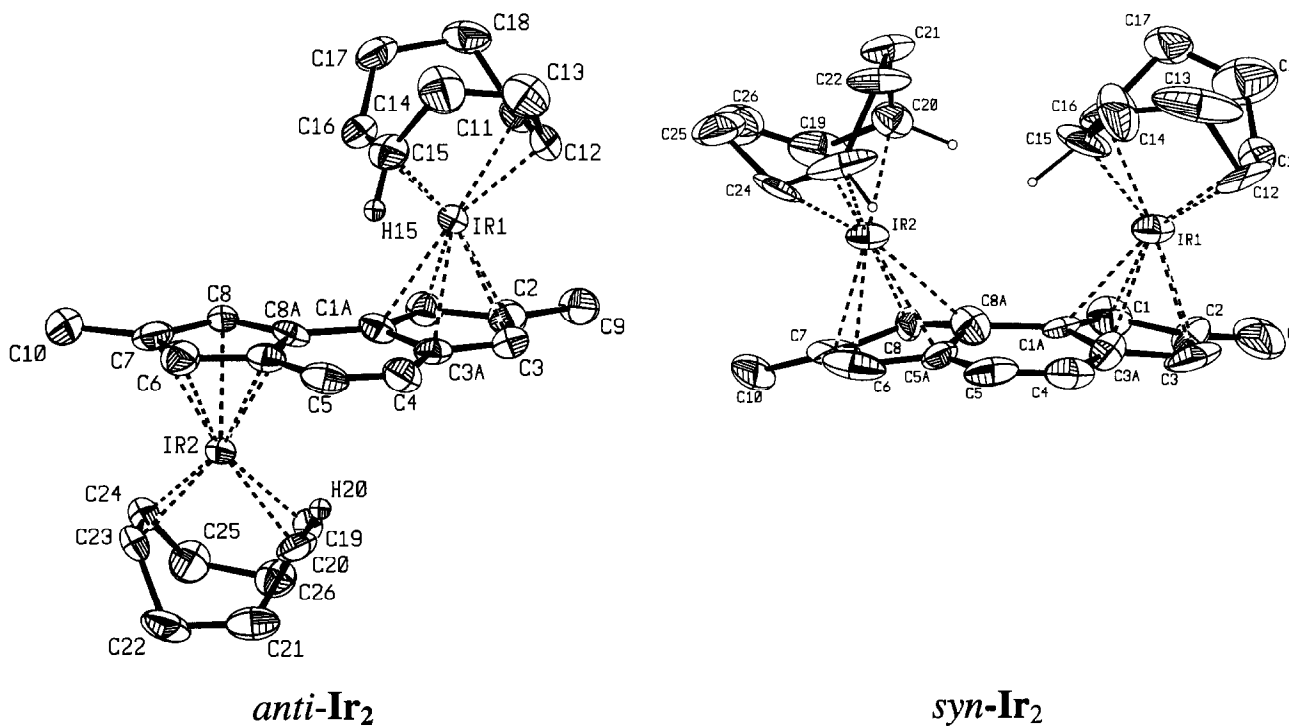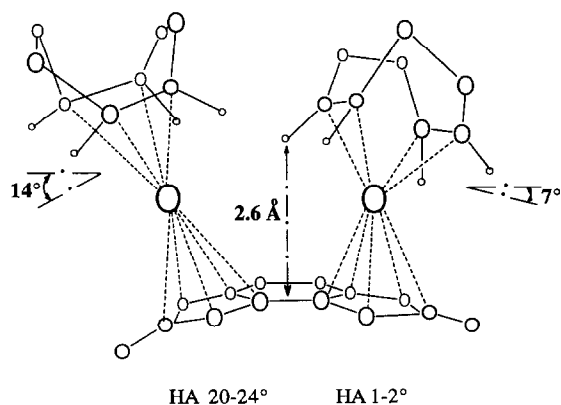

anti-**Ir₂**

syn-**Ir₂**

Fig. 2. ORTEP view of the structure of *anti*-{2,7-dimethyl-*as*-indacene-diide}-[Ir(COD)]₂} (*anti*-Ir₂), and *syn*-{2,7-dimethyl-*as*-indacene-diide}-[Ir(COD)]₂} (*syn*-Ir₂). The pertinent hydrogen atoms are evidenced.

HA 20-24°   HA 1-2°

Scheme 3. Schematic view of the structure of syn-{2,7-dimethyl-as-in-dacene-diide}-[Rh(COD)]₂} (syn-Rh₂). The hinge angles (HA [5]) of the two cyclopentadienyl rings and the distortions of the COD coordination versus rhodium are evidenced.

2.2. X-ray and NMR structural analysis

The structures of the homobimetallic *anti* and *syn* 2,7-dimethyl-*as*-indacene-diide complexes with Rh-(COD) (*syn*-Rh₂ and *anti*-Rh₂, respectively) and Ir-(COD) (*syn*-Ir₂ and *anti*-Ir₂) as determined by X-ray crystallographic analysis are shown in Figs. 1 and 2. The most relevant difference observed is the planar geometry (within 0.03 Å) of the bridging ligand in the *anti* complexes, whereas a noticeable deviation from the planarity for one of the cyclopentadienyl rings and, to a some extent, for the central benzene moiety is observed for the *syn* isomers, probably to avoid repulsive interactions between the COD groups. A simplified drawing of *syn*-Rh₂ structure is shown in Scheme 3.

Of particular interest is the conformation of these compounds with regard to the orientation of the COD ring. Actually, the conformation appears to be basically controlled by the following driving factors: (i) symmetry requirements, i.e. the necessity to achieve the highest symmetry consistent with the molecular constitution; this is always the determining factor in the case of monometallic, *syn* and *anti* heterobimetallic indenyl complexes [5] and monometallic *s*- or *as*-hydroindacenide complexes [11] (they show systematically the highest predictable symmetry or pseudosymmetry C_s); (ii) stereochemical hindrance, present mainly in the case of overcrowded *syn* binuclear indenide [5b,d] and indacene-diide derivatives [8,9]; (iii) the possibility of forming π-hydrogen bonds between the methine groups of COD and the arene π-electron systems present in the bridging ligand as reported recently for *anti*-{2,7-dimethyl-*as*-indacene-diide-[M(COD)]₂} [14].

Note that factor (iii) is never operative if there is the intrinsic possibility of satisfying condition (i), even though locally, as observed in the case of *s* or *as*-indacenide mononuclear complexes [11]. This fact cannot be regarded as a mere coincidence and we suggest the

leading role of factor (i), when present, to control the molecular conformation.

The structures described here confirm these findings. In Table 3 the most relevant geometrical parameters of *syn*-Rh₂ (and *syn*-Ir₂) compared with those of *anti*-Rh₂ (and *anti*-Ir₂) are reported. Scheme 4 displays the structure of the bridging ligand in the Rh complexes as evidenced by the pattern of bond distances.

This indicates a completely asymmetric molecular geometry in the *syn* derivatives and a degradation to the lower symmetry C_2 in the *anti* analogues, respectively. Thus, factor (iii) turns out to be the ruling force controlling the molecular structure of these compounds, the stereochemical factor (ii) being cooperative in the case of the complex *syn*-Rh₂ (and of *syn*-Ir₂).
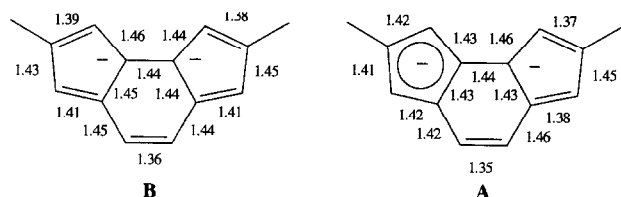
Table 3
Selected geometrical parameters for *anti*-{2,7-dimethyl-*as*-indacene-diide}-[Rh(COD)]₂} (**B**), *syn*-{2,7-dimethyl-*as*-indacene-diide}-[Rh(COD)]₂} (**A**), *anti*-{2,7-dimethyl-*as*-indacene-diide}-[Ir(COD)]₂} (**B′**), and *syn*-{2,7-dimethyl-*as*-indacene-diide}-[Ir(COD)]₂} (**A′**)

	A	A′	B	B′
M(1)–C(1)	2.28(1)	2.32(1)	2.277(8)	2.215(8)
M(1)–C(2)	2.24(1)	2.26(1)	2.243(9)	2.254(9)
M(1)–C(3)	2.15(1)	2.19(1)	2.28(1)	2.259(9)
M(1)–C(3a)	2.30(1)	2.25(1)	2.30(1)	2.296(7)
M(1)–C(1a)	2.29(1)	2.28(1)	2.252(9)	2.238(9)
M(2)–C(6)	2.23(1)	2.21(1)	2.26(1)	2.282(9)
M(2)–C(7)	2.23(1)	2.21(1)	2.28(1)	2.227(9)
M(2)–C(8)	2.20(1)	2.21(1)	2.30(1)	2.230(7)
M(2)–C(8a)	2.37(1)	2.37(1)	2.243(9)	2.257(7)
M(2)–C(5a)	2.35(1)	2.42(1)	2.238(8)	2.301(8)
C(1)–C(2)	1.37(2)	1.37(2)	1.382(9)	1.370(9)
C(1)–C(1a)	1.43(2)	1.46(2)	1.441(9)	1.459(9)
C(2)–C(3)	1.45(2)	1.46(2)	1.451(9)	1.460(9)
C(3)–C(3a)	1.38(2)	1.37(2)	1.412(9)	1.381(9)
C(3a)–C(4)	1.46(2)	1.44(2)	1.441(9)	1.459(9)
C(4)–C(5)	1.35(2)	1.32(2)	1.360(9)	1.320(9)
C(5)–C(5a)	1.42(2)	1.45(2)	1.45(1)	1.440(9)
C(5a)–C(6)	1.42(2)	1.41(2)	1.410(9)	1.377(8)
C(6)–C(7)	1.41(2)	1.43(2)	1.431(9)	1.449(9)
C(7)–C(8)	1.42(2)	1.43(2)	1.392(8)	1.371(8)
C(8)–C(8a)	1.43(2)	1.43(2)	1.460(9)	1.441(9)
C(8a)–C(1a)	1.44(2)	1.47(2)	1.441(9)	1.459(9)
C(8a)–C(5a)	1.41(2)	1.43(2)	1.450(9)	1.450(9)
C(3a)–C(1a)	1.43(2)	1.43(2)	1.442(9)	1.440(9)
C(2)–C(9)	1.53(2)	1.51(2)	1.520(8)	1.50(1)
H(15)···Q [a]	2.51	2.69	2.45	2.65
H(20)···Q [a]	–	–	2.40	2.60
Δ(M1–C) (Å) [b]	0.07	0.04	0.0	0.03
Δ(M2–C) (Å) [c]	0.19	0.20	0.01	0.02
HA(1) (°)	1	2	3	2
HA(1) (°)	20	24	2	3

[a] Q is the centroid of the six-membered ring of the arene ligand.
[b] Δ(M1–C) = {[(M1 − C₃ₐ) + (M1 − C₁ₐ)]/2 − [(M1 − C₁) + (M1 − C₂) + (M1 − C₃)]/3}.
[c] Δ(M2–C) = {[(M2 − C₈ₐ) + (M2 − C₅ₐ)]/2 − [(M2 − C₆) + (M2 − C₇) + (M2 − C₈)]/3}.

Scheme 4. The pattern of bond distances in syn-{2,7-dimethyl-as-in-dacene-diide}-[Rh(COD)]₂} **A**, and in anti-{2,7-dimethyl-as-indacene-diide}-[Rh(COD)]₂} **B**.

Table 4
Some intramolecular non-bonded distances (Å) for the anti-{2,7-dimethyl-as-indacene-diide}-[Rh(COD)]₂} (anti-Rh₂), and anti-{2,7-dimethyl-as-indacene-diide}-[Ir(COD)]₂} (anti-Ir₂), complexes

	anti-Rh₂	anti-Ir₂
C(20)–C(15)	3.47	3.50
C(20)–C(16)	3.56	3.64
C(21)–C(15)	3.53	3.58
C(28)–C(15)	3.51	3.55
H(20)–H(15)	2.18	2.22
H(20)–H(16)	2.15	2.14
H(20)–C(14)	2.60	2.55
H(20)–C(15)	2.62	2.60

As a matter of fact, in the syn isomers the COD ring bonded to the Rh(1) (or to the Ir(1) atom) is disposed with the olefin double bonds rotated about the axis through the metal and normal to the coordinated five-membered ring by ca. 60–70° with respect to that usually found [5]. In this way the observed interacting π-hydrogen bond with distances CH···Q of 2.51 Å (2.69 Å for the iridium derivative; Q is the centroid of the six-membered ring of the arene ligand) is realized, as found and described in detail in the cases of the anti species for both the COD rings [14]. In contrast, the COD ring bonded to Rh(2) in syn-Rh₂ and to Ir(2) in syn-Ir₂ assumes the usual conformation, i.e. that with the olefin double bonds orthogonal to the ring junction bond C(5a)–C(8a) [5], in order to avoid short intramolecular non-bonded distances (a few of them are nonetheless much shorter than would be expected from van der Waals radii, see Table 4). Identical conformations of the two COD rings would be severely hampered by stereochemical hindrance. To these conformations of the COD rings in syn-Rh₂ and syn-Ir₂ correspond quite different slip distortions and hinge angles (see Table 3): on the side of Rh(1) and Ir(1) they are almost annihilated by the counterbalancing π-hydrogen-bond interaction (as found also in anti-Rh₂ and anti-Ir₂); on the side of Rh(2) and Ir(2) these parameters are significantly larger than usually found [5] due to stereochemical repulsive effects between the two COD rings.

These results confirm the presence of π-hydrogen bonds in these molecules and offer a qualitative indication of their strength, which is evidently competitive with the energy involved in the slip and hinge angle distortions [5]. The higher reactivity of the syn isomers with respect to the anti isomers (see below) is then explainable in terms of an higher ground-state energy.

The NMR spectra of the homobimetallic complexes are expected to be quite simple in agreement with the molecular symmetry.
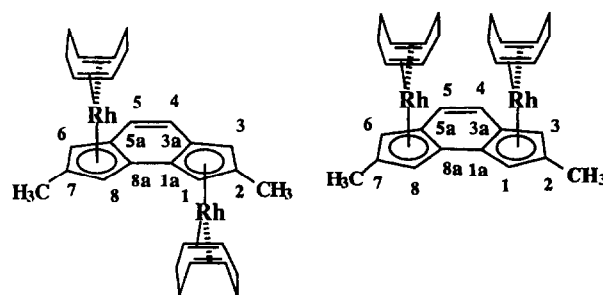
In fact, they show for each isomer one signal for the aromatic protons H(4) and H(5), one signal for the inner cyclopentadienyl protons H(1) and H(8), one signal for the outer analogues H(3) and H(6), and one signal for the methyl protons. The signals were assigned to the corresponding protons by NOESY measurements. As expected, the signals due to the olefin protons of COD are doubled by the intrinsic asymmetry of the bridging ligand. This asymmetry-induced chemical shift difference among these nuclei in the syn isomers, $\Delta\delta$ ca. 0.15 ppm, is very close to that observed for the corresponding monometallic 2,7-dimethyl-as-hydro-indacenide-M(COD) derivatives [11]. On the other hand, the value of the same parameter in the anti species is 0.52 ppm for anti-Rh₂ and 0.49 ppm for anti-Ir₂, the increased difference being due to the strong upfield shift of one of the resonances. On the basis of the crystallographic results, we attribute this phenomenon to the position of H(11) and H(20) protons which lie over the central six-membered ring, so that they are noticeably shielded by the ring currents induced by the static field in the π-electron cloud.

A similar characteristic has not been observed for the ¹³C spectra since the carbon nuclei C(11) and C(20) are outside of the anisotropy cone of the aromatic ring current. However, we observe that the chemical shift value of the inner quaternary carbon atoms C(1a) and C(8a) of the syn isomers (δ 107.1 for syn-Rh₂ and δ 101.7 for syn-Ir₂) is in the norm for such types of complexes [5], while in the anti isomers the same nuclei resonate markedly upfield (δ 99.5 in anti-Rh₂, and δ 94.2 in anti-Ir₂). Even this finding is in agreement with the π-electron distribution proposed on the basis of the

X-ray data and depicted in Scheme 4, where the limiting formula suggests for *anti*-Rh$_2$ and *anti*-Ir$_2$ an increased negative charge density in the (1a) and (8a) positions.

Finally, the magnetic equivalence exhibited by the two Cp rings of the *syn* isomers indicates that, at least in solution, there is fast exchange (on the NMR time scale) between the two different conformers determined in the crystal structure. This equivalence was observed even at low temperature (T 180 K).

2.3. Carbonylation of syn- and anti-{2,7-dimethyl-as-indacene-diide-[Rh(COD)]$_2$}

It has long been known that the ligand substitution reactions in indenyl metal complexes are significantly faster than in the analogous cyclopentadienyl compounds. This enhanced reactivity was attributed to an easier slippage from the η^5 towards a η^3 (or η^1) intermediate favored by the concomitant aromatization of the fused benzene ring (the *indenyl effect*) [15]. Preliminary attempts indicated that the carbonylation of the bimetallic *as*-indacene-diide-[M(COD)]$_2$ species (M = Rh, Ir) is even faster than that observed for the analogous monometallic indenyl–M(COD) compounds and it takes place in the temperature range of − 70 to − 30°C [16]. Our aim was to establish (i) whether the substitution of the two CODs occurs simultaneously or an intermediate mixed complex 2,7-dimethyl-*as*-indacene-diide-[M(CO)$_2$][M(COD)] is formed; (ii) if the *syn* and *anti* isomers exhibit the same reactivity.

Carbon monoxide was bubbled through a CH$_2$Cl$_2$ solution of a 2:1 mixture of *syn* and *anti*-2,7-dimethyl-*as*-indacene-diide-[Rh(COD)]$_2$ at − 78°C; portions of the reaction mixture were withdrawn at fixed times and analyzed for components by ^{1}H-NMR. After 10 min, a decrease of intensity of the signals due to the *syn* isomer with respect to an internal standard and no change for those of the *anti* reagent was observed. No signal due to the expected *syn* and *anti* tetracarbonyl products could be detected; a new set of signals appears at δ 6.881 and 6.836 (AB quartet, one H each), δ 5.674, 5.659, 5.133 and 5.001 (four multiplets, one H each), δ 2.396 and 2.266 (two singlets, three H each) together with two large multiplets at δ 4.033 and 3.427 (two H each). In this new set, the doubling of the NMR signals due to the protons of the bridging ligand with respect to the reagent indicates that the molecular symmetry is missed. The count of four (instead of the starting eight) for the olefin COD protons and the presence of two CO bands in the IR spectrum indicate that only one COD was replaced by two CO groups to yield the {2,7-dimethyl-*as*-indacene-diide-[η^5-Rh(CO)$_2$][η^5-Rh(COD)]}, *syn*-I, mixed complex, very likely in the *syn* geometry.

The presence of the strong π-acceptor Rh(CO)$_2$ group instead of the Rh(COD) one is supported by the

anti-I   syn-I
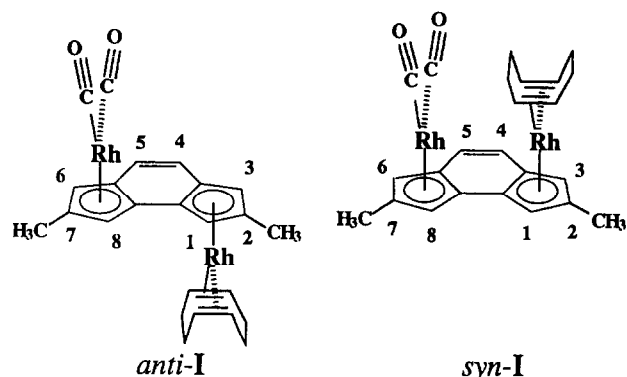
general downfield shift observed for the signals attributed to the indacene-diide skeleton, in particular for the resonances of one methyl group and of two cyclopentadienyl protons, which are assigned confidently to the five membered ring bonded to Rh(CO)$_2$. At longer reaction times (ca. 30′), the resonances due to the *anti* reagent decrease in intensity as well, and a new set of NMR signals appeared at δ 6.902 and 6.843 (AB quartet, one H each), δ 5.723, 5.676, 5.200 and 5.082 (four multiplets, one H each), δ 2.373 and 2.252 (two singlets, three H each) together with two large multiplets at δ 3.919 and 3.632 (two H each). At the same time, new stretching CO bands appeared in the IR spectrum. In analogy to what was discussed above, we believe that this new species is the intermediate *anti*-{2,7-dimethyl-*as*-indacene-diide-[η^5-Rh(CO)$_2$][η^5-Rh(COD)]}, *anti*-I, mixed complex, the trend of chemical shifts of which closely parallels that observed for the *syn*-I species.

At longer reaction times, both the *syn* and the *anti*-{2,7-dimethyl-*as*-indacene-diide-[η^5-Rh(CO)$_2$]$_2$} isomers are obtained in quantitative yields, as shown in Scheme 5.

No spectroscopic evidence for intermediates with rhodium η^1- or η^3-bonded to cyclopentadienyl rings was found even by running the synthetic experiment in the NMR tube at − 78°C.

This kinetic behavior is represented in Fig. 3 where the relative concentrations of reagents, the intermediates and the products have been reported versus time at − 78°C. The *syn* isomer reacts faster than the *anti* isomer; the mixed *syn* intermediate is produced, the concentration of which reached a maximum in a very short time; afterwards it decreased slowly. The concentration of the final *syn*-tetracarbonylated product increased steadily just from the early stages. Conversely, an induction period was observed for the formation of the *anti*-tetracarbonylated product due to the low concentration of the *anti* intermediate at the initial time. In conclusion, it appears that, in both the 2,7-dimethyl-*as*-indacene-diide-[Rh(COD)]$_2$ isomers, the substitution of the first COD is much faster than that of the second one. It follows that the presence of two CO molecules coordinated to one metal center (which in turn is η^5

bonded to the bridging ligand) influences the rate of substitution of the second COD unit. This result is a clear evidence of the existence of the *cooperative effect*, i.e. of electronic communication between the two metal centers mediated by the π-electron cloud of the bridging ligand. Therefore, a change of the electron density at one metal induced by changing the nature of the ancillary ligands changes the rate of substitution at the second metal significantly, the effect being whether the two metals are in the *syn* or in the *anti* disposition.

The factors responsible for the different reactivity exhibited by the two isomers in the first carbonylation step, can be probably referred mainly to their different ground state energies. As shown by the X-ray analysis, in fact, a higher energy of the *syn* complex may originate from the steric encumbrance between the two large Rh(COD) units which causes puckering and bowing of both the cyclopentadienyl and benzene rings as evidenced by the values of the hinge angle (HA, see Table 3 and Scheme 3). On the contrary, the *anti* complex is stabilized by π-hydrogen bonds and by a more pronounced aromatic character of the planar indacene-diide. To these ground-state energy differences, one needs to recall that relief of steric strain and planarization of the spacer might also favor the formation of the mixed *syn* intermediate with respect to the *anti* one.
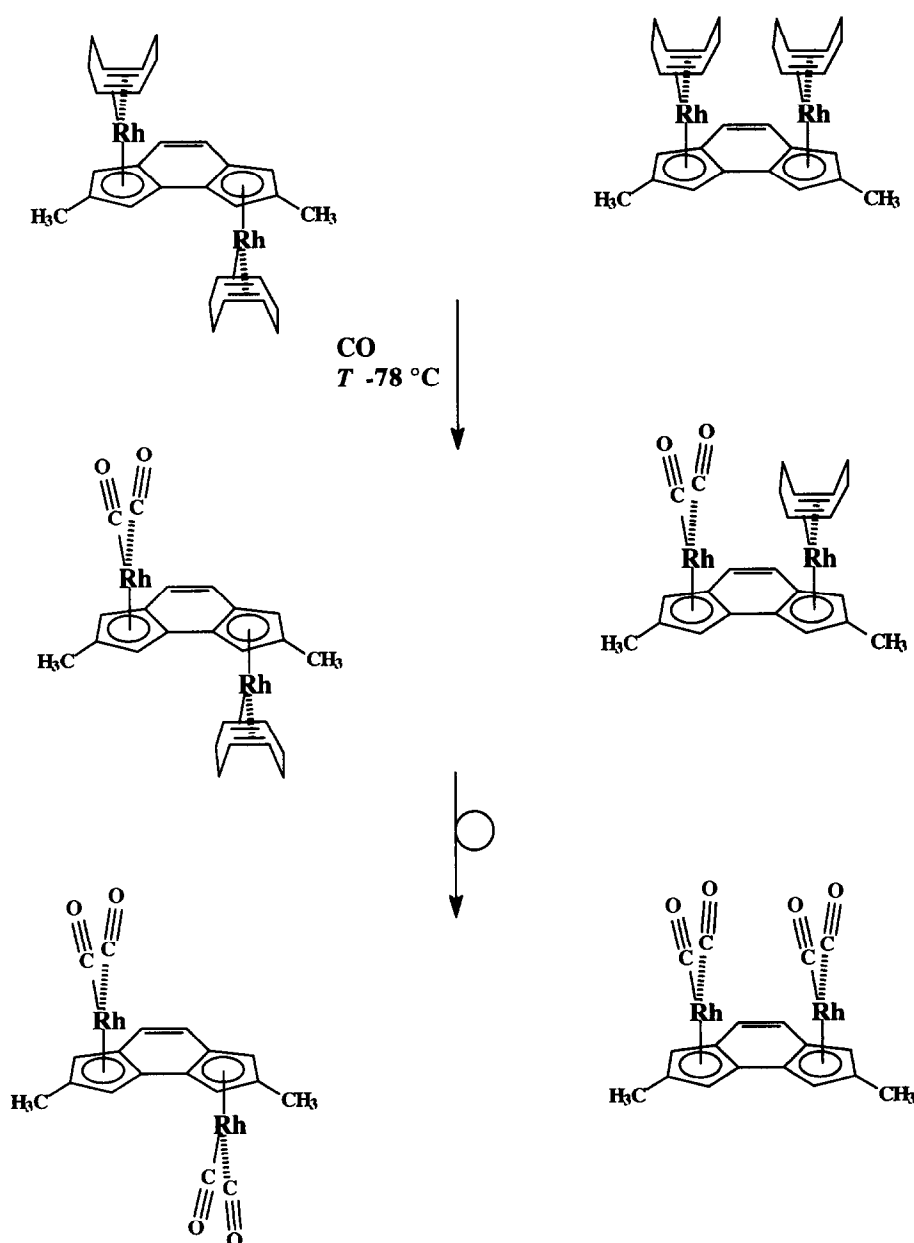
Scheme 5. The mechanism of carbonylation of *syn* and *anti*-{2,7-dimethyl-*as*-indacene-diide-[η^5-Rh(COD)]$_2$}.
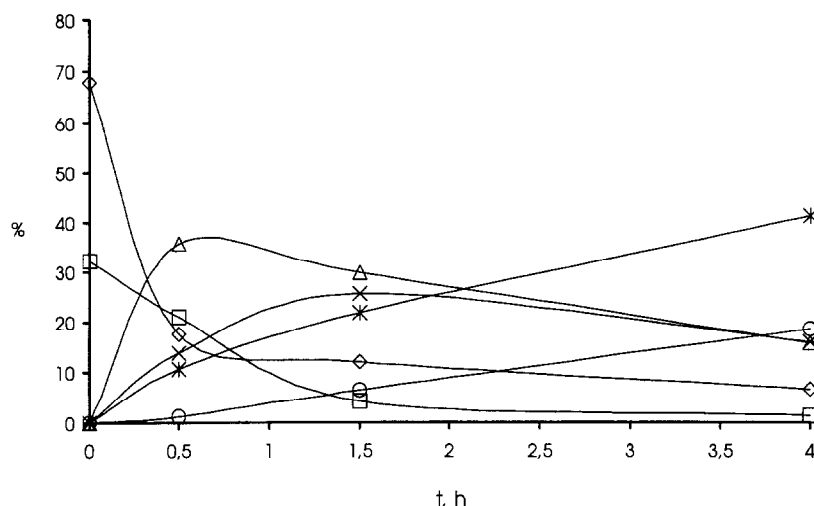
Fig. 3. Absolute percentages of the species involved in the carbonylation reaction of homobimetallic indacene-diide complexes of Rh(COD). T, $-78°C$; solvent, CH_2Cl_2. ◇, syn-{2,7-dimethyl-as-indacene-diide}-[Rh(COD)]$_2$}; □, anti-{2,7-dimethyl-as-indacene-diide}-[Rh(COD)]$_2$}; ×, anti-{2,7-dimethyl-as-indacene-diide}-[Rh(COD)][Rh(CO)$_2$]}; △, syn-{2,7-dimethyl-as-indacene-diide}-[Rh(COD)][Rh(CO)$_2$]}; *, syn-{2,7-dimethyl-as-indacene-diide}-[Rh(COD)][Rh(CO)$_2$]}; ○, anti-{2,7-dimethyl-as-indacene-diide}-[Rh(CO)$_2$]$_2$}.

2.4. Carbonylation of anti and syn-{2,7-dimethyl-as-indacene-diide-[Ir(COD)]$_2$}

Carbonylation of the syn and anti-{2,7-dimethyl-as-indacene-diide-[Ir(COD)]$_2$ complexes investigated under similar conditions revealed that the difference of reactivity between these isomers is noteworthy. In fact, NMR measurements indicated that below $-30°C$ the anti isomer is inert towards CO while the syn derivative reacts even at $-50°C$. Thus, after carbon monoxide is bubbled through a 2:1 mixture of the syn and anti isomers in CD_2Cl_2 at $-40°C$ for 1 h, it is observed in the ^1H spectrum that the resonances characteristic of the anti isomer remain unchanged, that the signals due to the syn reagent disappear and are substituted by a new set of resonances (see Section 3). By comparison with those observed for the (η^1-indenyl)-Ir(COD)(CO)$_2$ species [15], they were attributed to bimetallic iridium-indacenyl derivatives in which two Ir(COD)(CO)$_2$ groups are bonded to the cyclopentadienyl rings in an η^1 fashion as shown in the Scheme 6.

Thus, the first step of the carbonylation reaction consists in the fast addition of two COs to both the iridium atoms. No evidence for the addition to only one metal or the formation of mixed intermediates such as [Ir(COD)]-2,7-dimethyl-as-indacene-diide-[Ir(CO)$_2$] has been found. Moreover, we assume that the inorganic moieties maintain the syn geometry with respect to the mean plane of the bridging ligand. Out of the possible three isomers **A**, **B**, and **C** (see Scheme 7) that could be formed, only **A** and **B** in the ratio 2:1 have been detected and characterized by NOESY experiments. The chemical shift values are reported in Section 3. Likely, the third

possible isomer **C** is not formed and its instability could derive from steric interactions between the bulky [Ir(COD)(CO)$_2$] units.

At temperatures above $-20°C$ the CODs dissociate with simultaneous $\eta^1 \to \eta^5$ change of hapticity of both the iridium atoms towards cyclopentadienyls converting the bis-η^1 intermediates **A** and **B** into the tetracarbonylated species syn-{2,7-dimethyl-as-indacene-diide-[Ir(CO)$_2$]$_2$}. The values of chemical shift measured for this species are generally downfield with respect to those observed for the COD derivative, in good accordance with the enhanced π-acid character of CO versus COD. Since the carbonylation of the anti-{2,7-dimethyl-as-indacene-diide-[Ir(COD)]$_2$} isomer takes place at appreciable rate at temperatures above $-20°C$ only, no anti-bis-η^1 intermediates could be found due to their thermal instability. The anti-{2,7-dimethyl-as-indacene-diide-[Ir(CO)$_2$]$_2$} derivative is obtained in quantitative yield and the protons of this isomer, too, resonate downfield with respect to those of the COD precursor.

The IR spectra of the carbonylated species confirm their stereochemistry. In fact, only one of the two isomers (i.e. that present in the lowest quantity) exhibits two bands attributable to CO stretching in the two Ir(CO)$_2$ vibrators, viz., 2042 and 1966 cm^{-1} in CH_2Cl_2, and this finding is consistent with an anti disposition of the inorganic moieties. The other isomer exhibits four carbonyl bands in the same spectral region, viz., 2042, 2026, 1974, and 1959 cm^{-1} in the same solvent which is in agreement with two Ir(CO)$_2$ groups in a syn arrangement with respect to the bridging ligand. Similar results have been obtained for the syn and anti-{[Mn(CO)$_3$]$_2$-indacene-diide} isomers [9].

The different reactivity shown by the *syn* and *anti* bimetallic iridium isomers probably arises from the same structural factors invoked for the rhodium analogues which make the ground state of the *anti* isomer more stable than that of the *syn* one. The same factors do not seem to operate in the transition state, which should closely resemble the structure of the η¹ intermediate in which the aromaticity of the central benzene ring is restored and the two five membered rings have an indene-like structure. To the same structure one can trace back the lack of formation of the mixed carbonylated species, viz., {2,7-dimethyl-*as*-indacene-

diide-[Ir(CO)₂Ir(COD)]}, at a difference with the rhodium analogue. In fact, in the latter, every η¹ (or η³) intermediate (if any) formed during the carbonylation of the first Rh(COD) unit is transformed rapidly into the indacene-diide-[η⁵-Rh(CO)₂][η⁵-Rh(COD)] (it is worth noting that the low-hapticity rhodium–indenyl species are believed to be very unstable and they have never been spectroscopically observed so far [5]). In the mixed rhodium complex, the two η⁵-bonded metal atoms can communicate with each other through the bridging π-electron system so that the rate of the second carbonylation step is influenced by the
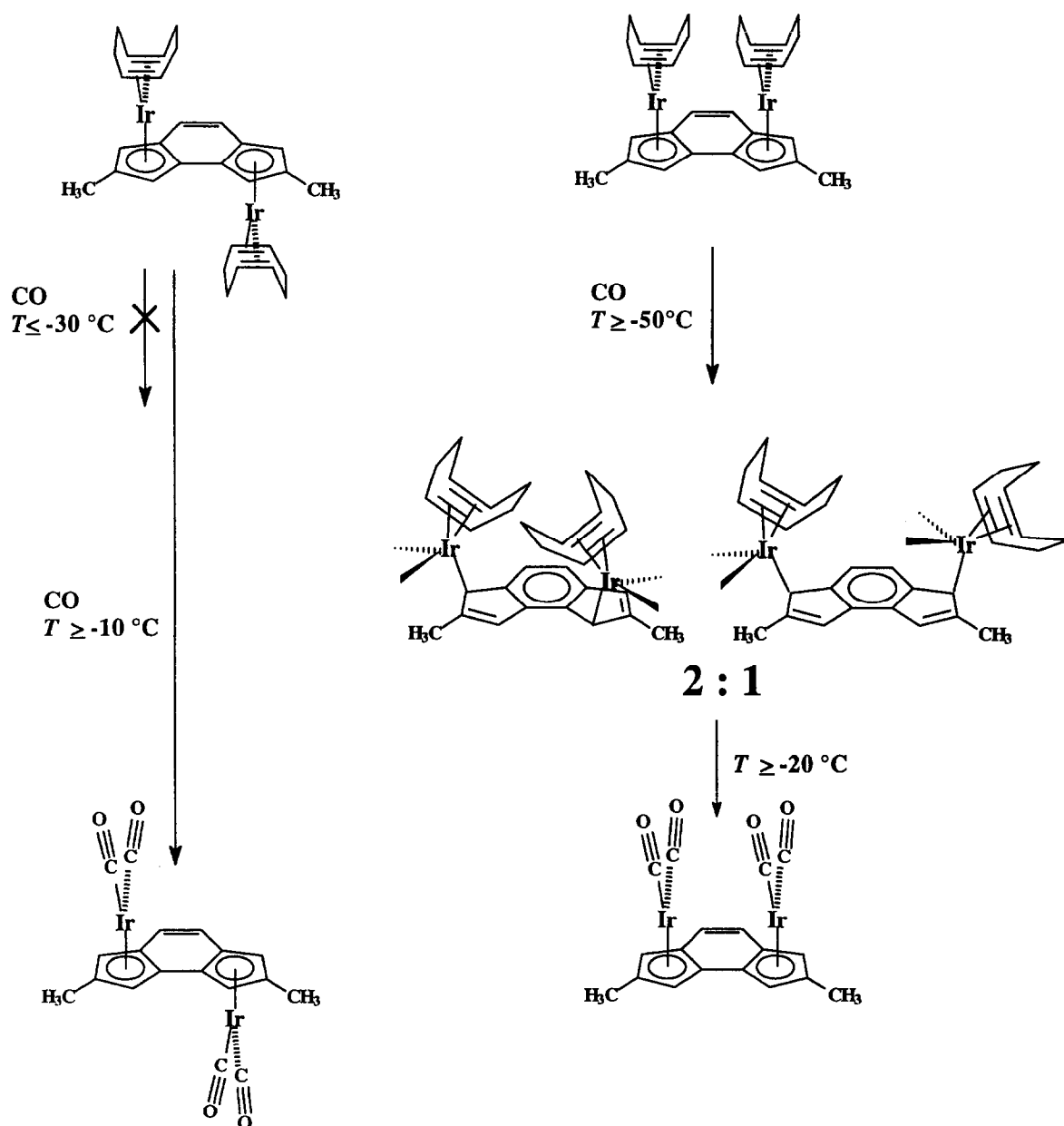
Scheme 6. The mechanism of carbonylation of *syn* and *anti*-{2,7-dimethyl-*as*-indacene-diide-[η⁵-Ir(COD)]₂}.
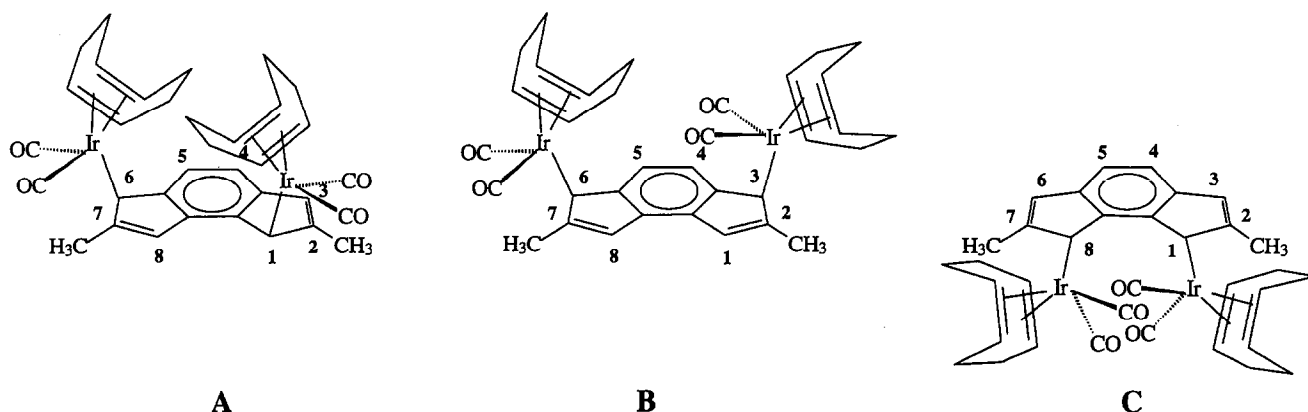
Scheme 7. The three possible bis-η^1 isomeric intermediate that could be formed in the carbonylation reaction of syn-{2,7-dimethyl-as-indacene-diide-[η^5-Ir(COD)]$_2$}.

diminished electron density at the second Rh(COD) center by the effect of COs bonded to the first rhodium. Conversely, in the carbonylation of the iridium derivative, the rapid addition of two COs per iridium atom affords the stable bis-η^1 intermediate. In this situation, the two metals, being connected to the bridging ligand through a σ bond, *do not communicate* through the bridge and they behave as two isolated inorganic moieties. In fact, a very similar spectroscopic behavior was observed when monometallic indenyl– [16] and hydroindacenide–Ir(COD) [17] derivatives have been carbonylated under identical conditions.

3. Experimental

3.1. General

All reactions and complex manipulations were performed in an oxygen- and moisture-free atmosphere. The solvents were dried carefully and deoxygenated before use. The complexes appear as microcrystalline air-stable powders, which gave satisfactory elemental analysis. Melting points are uncorrected. Microanalyses were performed at the Dipartimento di Chimica Inorganica, Metallorganica ed Analitica, Università di Padova. The IR spectra were recorded as THF solutions on a Perkin–Elmer 1600 FTIR spectrometer, and the 70 eV electron impact mass spectra were measured with a VG 16 Micromass spectrometer. The ^{1}H- and ^{13}C-NMR spectra were obtained as CDCl$_3$ or CD$_2$Cl$_2$ solutions on a Bruker DRX-400 spectrometer operating at 400.13 and 100.61 MHz, respectively. The assignments of the proton resonances were performed by standard chemical shift correlations and COSY and NOESY experiments. Those of ^{13}C were performed by 2D-heterocorrelated COSY (HMQC with *bird* sequence [18] and quadrature along F1 achieved using the TPPI

method [19] for the H-bonded carbon atoms, HMBC [20] for the quaternary ones).

3.2. Synthesis of the ligands

The ligands s-dihydro-indacene (1) (obtained as a mixture of the 1,5- and 1,7 isomers) [21], 2,6-dimethyl-1,7-dihydro-s-indacene (2) [9], and 2,7-dimethyl-1,6-dihydro-as-indacene (3) [9] were obtained with the quoted methods. The physical properties agree with those reported, and an updated set of the NMR parameters, obtained by 1D spectra and 2D homo and heteronuclear correlations, has been reported recently [11].

3.3. Bis-metallation reaction

To a well-stirred solution of the appropriate ligand in anhydrous, oxygen-free THF kept at −20 to −30°C, two equivalents of *t*-butyl lithium in pentane were added to produce the corresponding dianion. After a few minutes, the solution was added to two equivalents of the metal dimer dissolved in anhydrous THF kept at −30°C. After an additional 20 min of stirring, the solvents were pumped off at −30°C and the residue analyzed by NMR to obtain the products ratio. The crude mixture was then extracted with anhydrous CH$_2$Cl$_2$, filtered carefully and evaporated to dryness.

3.4. s-Indacene-diide-[Rh(COD)]$_2$

Yield, 80–90%. *Syn/anti* ratio, 9:1. *Syn* isomer: ^{1}H-NMR (CD$_2$Cl$_2$, *T* 298 K, ppm from internal TMS): δ 6.98 (s, 2H, H$_{4,8}$) 6.15 (q, 2H, J(H$_{1,2}$) = J(H$_{2,3}$) = J(^{103}Rh-H$_2$) 2.6 Hz, H$_{2,6}$), 5.13 (d, 4H, 2H, J(H$_{1,2}$) = J(H$_{2,3}$) 2.6 Hz, H$_{1,3,5,7}$), 4.22 (m, 8H, J(^{103}Rh-H$_2$) ca. 2 Hz, COD olefin protons), and 2.0–1.8 (m, 16H, COD methylene protons). ^{13}C-NMR (*T* 273 K): δ 118.50 (4C,

$J(^{103}Rh-^{13}C)$ 1.7 Hz, $C_{2a,3a,7a,8a}$), 98.41 (2C, $C_{4,8}$), 94.74 (2C, $J(^{103}Rh-^{13}C)$ 6.5 Hz, $C_{2,6}$), 74.39 (4C, $J(^{103}Rh-^{13}C)$ 4.6 Hz, $C_{1,3,5,7}$), 69.48 (8C, $J(^{103}Rh-^{13}C)$ 13.2 Hz, COD olefin carbons), and 31.83 (16C, COD methylene carbons). *Anti* isomer: ¹H-NMR (CD₂Cl₂, T 298 K, ppm from internal TMS): δ 6.88 (s, 2H, $H_{4,8}$) 6.18 (q, 2H, $J(H_{1,2}) = J(H_{2,3}) = J(^{103}Rh-H_2)$ 2.9 Hz, $H_{2,6}$), 5.15 (d, 4H, 2H, $J(H_{1,2}) = J(H_{2,3})$ 2.9 Hz, $H_{1,3,5,7}$), 4.01 (m, 8H, $J(^{103}Rh-H_2)$ ca. 2 Hz, COD olefin protons), and 1.9–1.7 (m, 16H, COD methylene protons). The ¹³C-NMR was not obtained by the very low concentration of the species.

3.5. s-Indacene-diide-[Ir(COD)]₂

Yield, 23%. *Syn/anti* ratio, 9:1. *Syn* isomer: ¹H-NMR (CD₂Cl₂, T 298 K, ppm from internal TMS): δ 7.14 (s, 2H, $H_{4,8}$) 6.07 (t, 2H, $J(H_{1,2}) = J(H_{2,3})$ 2.3 Hz, $H_{2,6}$), 5.33 (d, 4H, 2H, $J(H_{1,2}) = J(H_{2,3})$ 2.3 Hz, $H_{1,3,5,7}$), 4.15 (m, 8H, COD olefin protons), and 1.8–1.6 (m, 16H, COD methylene protons). ¹³C-NMR (T 273 K): δ 116.62 (4C, $C_{3a,4a,7a,8a}$), 108.20 (2C, $C_{4,8}$), 87.41 (2C, $C_{2,6}$), 69.30 (4C, $C_{1,3,5,7}$), 52.89 (8C, COD olefin carbons), and 31.13 (16C, COD methylene carbons). *Anti* isomer: ¹H-NMR (CD₂Cl₂, T 298 K, ppm from internal TMS): δ 7.05 (s, 2H, $H_{4,8}$) 5.86 (t, 2H, $J(H_{1,2}) = J(H_{2,3})$ 2.4 Hz, $H_{2,6}$), 5.19 (d, 4H, 2H, $J(H_{1,2}) = J(H_{2,3})$ 2.4 Hz, $H_{1,3,5,7}$), 4.15 (m, 8H, COD olefin protons), and 1.8–1.6 (m, 16H, COD methylene protons). The ¹³C-NMR was not obtained by the very low concentration of the species.

3.6. s-Indacene-diide-[Rh(NBD)]₂

Yield, 65%. *Syn/anti* ratio, 4.5:1. *Syn* isomer: ¹H-NMR (CD₂Cl₂, T 298 K, ppm from internal TMS): δ 7.13 (s, 2H, $H_{4,8}$) 6.07 (q, 2H, $J(H_{1,2}) = J(H_{2,3})$ 2.8 Hz, $J(^{103}Rh-H_2)$ 2.2 Hz, $H_{2,6}$), 5.19 (d, 4H, 2H, $J(H_{1,2}) = J(H_{2,3})$ 2.8 Hz, $H_{1,3,5,7}$), 3.60 (m, 8H, NBD olefin protons), 3.36 (m 4H, NBD bridgehead protons), and 0.97 (t, 2H, NBD methylene protons). ¹³C-NMR (T 273 K): δ 110.63 (4C, $J(^{103}Rh-^{13}C)$ 1.8 Hz, $C_{3a,4a,7a,8a}$), 106.35 (2C, $C_{4,8}$), 93.23 (2C, $J(^{103}Rh-^{13}C)$ 6.2 Hz, $C_{2,6}$), 71.50 (4C, $J(^{103}Rh-^{13}C)$ 5.4 Hz, $C_{1,3,5,7}$), 59.07 (2C, $J(^{103}Rh-^{13}C)$ 6.2 Hz, NBD methylene carbons), 49.31 (4C, $J(^{103}Rh-^{13}C)$ 2.7 Hz, NBD bridgehead carbons), and 42.90 (8C, $J(^{103}Rh-^{13}C)$ 9.8 Hz, NBD olefin carbons). *Anti* isomer: ¹H-NMR (CD₂Cl₂, T 298 K, ppm from internal TMS): δ 6.94 (s, 2H, $H_{4,8}$) 6.22 (q, 2H, $J(H_{1,2}) = J(H_{2,3})$ 2.9 Hz, $J(^{103}Rh-H_2)$ 2.4 Hz, $H_{2,6}$), 5.13 (d, 4H, 2H, $J(H_{1,2}) = J(H_{2,3})$ 2.9 Hz, $H_{1,3,5,7}$), 3.47 (2H, m, NBD bridgehead protons), 3.18 (m, 8H, NBD olefin protons), and 0.89 (t, 4H, NBD methylene protons). The ¹³C-NMR was not obtained by the very low concentration of the species.

3.7. s-Indacene-diide-[Rh(η²-C₂H₄)₂]₂

Yield, 40%. *Syn/anti* ratio, 1.5:1. *Syn* isomer: ¹H-NMR (CD₂Cl₂, T 298 K, ppm from internal TMS): δ 7.03 (s, 2H, $H_{4,8}$) 6.32 (q, 2H, $J(H_{1,2}) = J(H_{2,3})$ 2.8 Hz, $J(^{103}Rh-H_2)$ 2.7 Hz, $H_{2,6}$), 5.13 (d, 4H, 2H, $J(H_{1,2}) = J(H_{2,3})$ 2.8 Hz, $H_{1,3,5,7}$), 2.20 (d, 16H, $J(^{103}Rh-H)$ 2.0 Hz, ethylene protons). ¹³C-NMR (T 273 K): δ 115.86 (4C, $J(^{103}Rh-^{13}C)$ ca. 1.5 Hz, $C_{3a,4a,7a,8a}$), 106.55 (2C, $C_{4,8}$), 94.13 (2C, $C_{2,6}$), 77.45 (4C, $C_{1,3,5,7}$), and 47.15 (broad signal, 16C, ethylene carbons). *Anti* isomer: ¹H-NMR (CD₂Cl₂, T 298 K, ppm from internal TMS): δ 7.25 (s, 2H, $H_{4,8}$) 6.16 (q, 2H, $J(H_{1,2}) = J(H_{2,3})$ 2.9 Hz, $J(^{103}Rh-H_2)$ 2.5 Hz, $H_{2,6}$), 5.27 (d, 4H, 2H, $J(H_{1,2}) = J(H_{2,3})$ 2.9 Hz, $H_{1,3,5,7}$), 2.31 (d, 16H, $J(^{103}Rh-H)$ 2.2 Hz, ethylene protons). ¹³C-NMR (T 273 K): δ 115.63 (4C, $J(^{103}Rh-^{13}C)$ ca. 1.5 Hz, $C_{3a,4a,7a,8a}$), 105.46 (2C, $C_{4,8}$), 93.32 (2C, $C_{2,6}$), 77.13 (4C, $C_{1,3,5,7}$), and 46.57 (broad signal, 16C, ethylene carbons).

3.8. s-Indacene-diide-[Rh(CO)₂]₂

Yield, 40%. *Syn/anti* ratio, 1:19. *Syn* isomer: ¹H-NMR (CD₂Cl₂, T 298 K, ppm from internal TMS): δ 7.19 (s, 2H, $H_{4,8}$) 6.17 (q, 2H, $J(H_{1,2}) = J(H_{2,3})$ 2.9 Hz, $J(^{103}Rh-H_2)$ 2.8 Hz, $H_{2,6}$), 5.81 (d, 4H, 2H, $J(H_{1,2}) = J(H_{2,3})$ 2.9 Hz, $H_{1,3,5,7}$). ¹³C-NMR (T 298 K): δ 189.75 (2C d, $J(^{103}Rh-^{13}C)$ 86.4 Hz, C≡O), 120.07 (4C, $J(^{103}Rh-^{13}C)$ 1.2 Hz, $C_{3a,4a,7a,8a}$), 107.11 (2C, $C_{4,8}$), 101.27 (2C, $J(^{103}Rh-^{13}C)$ 6.6 Hz, $C_{2,6}$), and 75.01 (4C, $J(^{103}Rh-^{13}C)$ 3.8 Hz, $C_{1,3,5,7}$). *Anti* isomer: ¹H-NMR (CD₂Cl₂, T 298 K, ppm from internal TMS): δ 7.01 (s, 2H, $H_{4,8}$) 6.22 (q, 2H, $J(H_{1,2}) = J(H_{2,3})$ 3.1 Hz, $J(^{103}Rh-H_2)$ 2.8 Hz, $H_{2,6}$), and 5.81 (d, 4H, 2H, $J(H_{1,2}) = J(H_{2,3})$ 3.1 Hz, $H_{1,3,5,7}$). ¹³C-NMR (T 298 K): δ 189.99 (2C d, $J(^{103}Rh-^{13}C)$ 86.3 Hz, C≡O), 120.63 (4C, $J(^{103}Rh-^{13}C)$ 1.4 Hz, $C_{3a,4a,7a,8a}$), 107.19 (2C, $C_{4,8}$), 100.88 (2C, $J(^{103}Rh-^{13}C)$ 6.7 Hz, $C_{2,6}$), and 74.81 (4C, $J(^{103}Rh-^{13}C)$ 3.4 Hz, $C_{1,3,5,7}$).

3.9. 2,6-Dimethyl-s-indacene-diide-[Rh(COD)]₂

Yield, 80–90%. *Syn/anti* ratio, 7:1. *Syn* isomer: ¹H-NMR (CD₂Cl₂, T 298 K, ppm from internal TMS): δ 6.74 (s, 2H, $H_{4,8}$), 5.01 (m, 4H, $H_{1,3,5,7}$), 4.17 (m, 8H, $J(^{103}Rh-H_2)$ ca. 2 Hz, COD olefin protons), 2.34 (d, 6H, $J(^{103}Rh-H)$ 2.2 Hz, 2,6-(CH₃)), and 2.0–1.8 (m, 16H, COD methylene protons). ¹³C-NMR (T 273 K): δ 117.66 (4C, $J(^{103}Rh-^{13}C)$ ca. 1 Hz, $C_{3a,4a,7a,8a}$), 106.07 (2C, $C_{4,8}$), 76.34 (4C, $J(^{103}Rh-^{13}C)$ 5.0 Hz, $C_{1,3,5,7}$), 69.20 (8C, $J(^{103}Rh-^{13}C)$ 13.4 Hz, COD olefin carbons), 31.81 (16C, COD methylene carbons) and 15.89 (s, 2C, 2-6-(CH₃). *Anti* isomer: ¹H-NMR (CD₂Cl₂, T 298 K, ppm from internal TMS): δ 6.65 (s, 2H, $H_{4,8}$), 5.03 (m, 4H, $H_{1,3,5,7}$), 4.00 (m, 8H, $J(^{103}Rh-H_2)$ ca. 2 Hz, COD olefin protons), 2.39 (d, 6H, $J(^{103}Rh-H$ 2.2 Hz, 2-6-(CH₃)), and 2.0–1.7

(m, 16H, COD methylene protons). ^{13}C-NMR (T 273 K): δ 116.50 (4C, $J(^{103}$Rh$-^{13}$C) ca. 1 Hz, $C_{3a,4a,7a,8a}$), 105.76 (2C, $C_{4,8}$), 76.25 (4C, $J(^{103}$Rh$-^{13}$C) 4.3 Hz, $C_{1,3,5,7}$), 69.02 (8C, $J(^{103}$Rh$-^{13}$C) 13.6 Hz, COD olefin carbons), 31.26 (16C, COD methylene carbons) and 15.76 (s, 2C, 2-6-(CH$_3$).

3.10. 2,6-Dimethyl-s-indacene-diide-[Ir(COD)]₂

Yield, 25%. *Syn/anti* ratio, 9:1. *Syn* isomer: ^{1}H-NMR (CD$_2$Cl$_2$, T 298 K, ppm from internal TMS): δ 6.92 (s, 2H, H$_{4,8}$), 5.21 (m, 4H, H$_{1,3,5,7}$), 4.09 (m, 8H, COD olefin protons), 2.29 (s, 6H, 2,6-(CH$_3$)), and 1.8–1.6 (m, 16H, COD methylene protons). *Anti* isomer: ^{1}H-NMR (CD$_2$Cl$_2$, T 298 K, ppm from internal TMS): δ 6.79 (s, 2H, H$_{4,8}$), 5.20 (m, 4H, H$_{1,3,5,7}$), 3.97 (m, 8H, COD olefin protons), 2.36 (s, 6H, 2-6-(CH$_3$)), and 1.8–1.6 (m, 16H, COD methylene protons).

3.11. as-Indacene-diide-[Rh(COD)]₂

Yield, 80–90%. *Syn/anti* ratio: 3:1. *Syn* isomer: ^{1}H-NMR (CD$_2$Cl$_2$, T 298 K, ppm from internal TMS): δ 6.92 (m, 2H, H$_{4,5}$), 5.91 (m, 2H, J(Rh–H) 2.0 Hz, H$_{2,7}$), 5.28 (m, 2H, H$_{3,6}$), 4.98 (m, 2H, H$_{1,8}$), 4.20 and 4.06 (2m, 4H each, olefin protons of COD), and 2.2–1.6 (m, 16H, methylene protons of COD). ^{13}C-NMR (T 298 K): δ 117.44 (2C, C$_{4,5}$), 108.85 (2C, $J(^{103}$Rh$-^{13}$C) 2.8 Hz, C$_{3a,5a}$), 108.81 (2C, $J(^{103}$Rh$-^{13}$C) 2.5.5 Hz, C$_{1a,8a}$), 89.84 (2C, $J(^{103}$Rh$-^{13}$C) 4.1 Hz, C$_{2,7}$), 77.66 (2C, $J(^{103}$Rh$-^{13}$C) 4.8 Hz, C$_{3,6}$), 77.06 (2C, $J(^{103}$Rh$-^{13}$C) 3.7 Hz, C$_{1,8}$), 67.43 and 66.55 (4C each, $J(^{103}$Rh$-^{13}$C) 14.7 and 13.5 Hz, olefin carbons of COD), and 34.60 and 30.21 (4C each, methylene carbons of COD). *Anti* isomer: ^{1}H-NMR (CD$_2$Cl$_2$, T 298 K, ppm from internal TMS): δ 6.98 (m, 2H, H$_{4,5}$), 5.85 (m, 2H, J(Rh–H) 1.6 Hz, H$_{2,7}$), 5.18 (m, 2H, H$_{3,6}$), 5.16 (m, 2H, H$_{1,8}$), 3.92 and 3.61 (2m, 4H each, olefin protons of COD), and 2.2/1.8 (m, 16H, methylene protons of COD). ^{13}C-NMR (T 298 K): δ 116.19 (2C, C$_{4,5}$), 107.08 (2C, $J(^{103}$Rh$-^{13}$C) 2.5 Hz, C$_{3a,5a}$), 101.59 (2C, $J(^{103}$Rh$-^{13}$C) 2.4 Hz, C$_{1a,8a}$), 88.55 (2C, $J(^{103}$Rh$-^{13}$C) 4.9 Hz, C$_{2,7}$), 79.22 (2C, $J(^{103}$Rh$-^{13}$C) 4.9 Hz, C$_{3,6}$), 76.29 (2C, $J(^{103}$Rh$-^{13}$C) 3.7 Hz, C$_{1,8}$), 67.96 and 66.65 (4C each, $J(^{103}$Rh$-^{13}$C) 14.3 and 14.4 Hz, olefin carbons of COD), and 32.38 and 31.98 (4C each, methylene carbons of COD).

3.12. as-Indacene-diide-[Rh(NBD)]₂

Yield, 45%. *Syn/anti* ratio: 3.1. *Syn* isomer: ^{1}H-NMR (CD$_2$Cl$_2$, T 298 K, ppm from internal TMS): δ 6.98 (m, 2H, H$_{4,5}$), 5.70 (m, 2H, J(Rh–H) ca. 2 Hz, H$_{2,7}$), 5.34 (m, 2H, H$_{1,8}$), 5.23 (m, 2H, H$_{3,6}$), 3.39 and 3.33 (2m, 4H each, olefin protons of NBD), 3.32 (m, 4H, NBD bridgehead protons), and 0.92 (t, 4H, methylene pro-

tons of NBD). ^{13}C-NMR (T 298 K): δ 117.98 (2C, C$_{4,5}$), 105.23 (2C, C$_{3a,7a}$), 103.82 (2C, C$_{1a,8a}$), 86.83 (2C, C$_{2,7}$), 77.72 (2C, $J(^{103}$Rh$-^{13}$C) ca. 5 Hz, C$_{3,6}$), 75.34 (2C, $J(^{103}$Rh$-^{13}$C) 4.2 Hz, C$_{1,8}$), 56.73 (2C each, $J(^{103}$Rh$-^{13}$C) 6.7 Hz, methylene carbon of NBD), 48.01 and 47.94 (4C each, $J(^{103}$Rh$-^{13}$C) ca. 2 Hz, bridgehead carbons of NBD), 34.66 and 33.89 (4C each, $J(^{103}$Rh$-^{13}$C) 10.2 Hz, olefin carbons of NBD). *Anti* isomer: ^{1}H-NMR (CD$_2$Cl$_2$, T 298 K, ppm from internal TMS): δ 6.82 (m, 2H, H$_{4,5}$), 5.76 (m, 2H, J(Rh–H) ca. 2 Hz, H$_{2,7}$), 5.22 (m, 2H, H$_{1,8}$), 5.17 (m, 2H, H$_{3,6}$), 3.13 (m, 4H, NBD bridgehead protons), 3.15 and 2.85 (2m, 4H each, olefin protons of NBD), and 0.78 (t, 4H, methylene protons of NBD). ^{13}C-NMR (T 298 K): δ 116.67 (2C, C$_{4,5}$), 104.67 (2C, $J(^{103}$Rh$-^{13}$C) ca. 3 Hz, C$_{3a,5a}$), 99.36 (2C, $J(^{103}$Rh$-^{13}$C) ca. 2 Hz, C$_{1a,8a}$), 86.60 (2C, $J(^{103}$Rh$-^{13}$C) 5.4 Hz, C$_{2,7}$, 78.02 (2C, $J(^{103}$Rh$-^{13}$C) ca. 4 Hz, C$_{1,8}$), 74.11 (2C, $J(^{103}$Rh$-^{13}$C) 4.3 Hz, C$_{3,6}$), 57.41 (2C, $J(^{103}$Rh$-^{13}$C) 6.7 Hz, methylene carbon of NBD), 47.32 and 47.25 (4C each, $J(^{103}$Rh$-^{13}$C) 2.4 Hz, bridgehead carbons of NBD), 34.80 and 33.95 (4C each, $J(^{103}$Rh$-^{13}$C) 10.5 Hz, olefin carbons of NBD).

3.13. as-Indacene-diide-[Rh(η^2-C₂H₄)₂]₂

Yield, 40%. *Syn/anti* ratio: 2:1. *Syn* isomer: ^{1}H-NMR (CD$_2$Cl$_2$, T 298 K, ppm from internal TMS): δ 7.08 (m, 2H, H$_{4,5}$), 6.00 (m, 2H, J(Rh–H) ca. 2 Hz, H$_{2,7}$), 5.17 (m, 2H, H$_{1,8}$), 5.15 (m, 2H, H$_{3,5}$), 2.8 and 2.0 (broad signals, 16H overall, ethylene protons). ^{13}C-NMR (T 298 K): δ 117.17 (2C, C$_{4,5}$), 104.1 (2C, $J(^{103}$Rh$-^{13}$C) ca. 3 Hz, C$_{3a,5a}$), 102.8 (2C, $J(^{103}$Rh$-^{13}$C) ca. 3 Hz, C$_{1a,8a}$), 88.82 (2C, $J(^{103}$Rh$-^{13}$C) ca. 4 Hz, C$_{2,7}$), 81.70 (2C, $J(^{103}$Rh$-^{13}$C) ca. 3 Hz, C$_{3,6}$), 78.26 (2C, $J(^{103}$Rh$-^{13}$C) ca. 4 Hz, C$_{1,8}$), and 43.00 (8C, $J(^{103}$Rh$-^{13}$C 13.6 Hz, ethylene carbons). *Anti* isomer: ^{1}H-NMR (CD$_2$Cl$_2$, T 298 K, ppm from internal TMS): δ 6.85 (m, 2H, H$_{4,5}$), 5.72 (m, 2H, J(Rh–H) ca. 2 Hz, H$_{2,7}$), 5.49 (m, 2H, H$_{1,8}$), 5.32 (m, 2H, H$_{3,6}$), 2.8 and 2.0 (broad signals, 16H overall, ethylene protons). ^{13}C-NMR (T 298 K): δ 119.14 (2C, C$_{4,5}$), 104.5 (2C, $J(^{103}$Rh$-^{13}$C) 4.3 Hz, C$_{3a,5a}$), 99.01 (2C, $J(^{103}$Rh$-^{13}$C) ca. 2 Hz, C$_{1a,8a}$), 89.01 (2C, $J(^{103}$Rh$-^{13}$C) 4.2 Hz, C$_{2,7}$), 81.25 (2C, $J(^{103}$Rh$-^{13}$C) ca. 4 Hz, C$_{3,6}$), 78.24 (2C, $J(^{103}$Rh$-^{13}$C) ca. 4 Hz, C$_{1,8}$), and 42.50 (8C, $J(^{103}$Rh$-^{13}$C) 13.6 Hz, ethylene carbons).

3.14. as-Indacene-diide-[Rh(CO)₂]₂

Yield, 76%. *Syn/anti* ratio: 1:5. *Syn* isomer: ^{1}H-NMR (CD$_2$Cl$_2$, T 298 K, ppm from internal TMS): δ 7.15 (m, 2H, H$_{4,5}$), 6.26 (m, 2H, H$_{1,8}$). 6.12 (m, 2H, J(Rh–H) ca. 3 Hz, CH$_{2,7}$), 5.64 (m, 2H, H$_{3,6}$), and ^{13}C-NMR (T 298 K): δ 117.24 (2C, C$_{4,5}$), 115.20 (2C, $J(^{103}$Rh$-^{13}$C ca. 4 Hz, C$_{3a,5a}$), 105.51 (2C, $J(^{103}$Rh$-^{13}$C ca. 2 Hz, C$_{1a,8a}$),

96.89 (2C, $J(^{103}Rh-^{13}C)$ 3.5 Hz, $C_{2,7}$), 76.64 (2C, $J(^{103}Rh-^{13}C)$ 3.5 Hz, $C_{3,6}$), and 75.30 (2C, $J(^{103}Rh-^{13}C)$ 3.4 Hz, $C_{1,8}$). *Anti* isomer: ^{1}H-NMR (CD$_2$Cl$_2$, T 298 K, ppm from internal TMS): δ 7.15 (m, 2H, H$_{4,5}$), 6.14 (m, 2H, J(Rh–H) ca. 3 Hz, H$_{2,7}$) 5.85 (m, 2H, H$_{1,8}$), 5.71 (m, 2H, H$_{3,6}$). ^{13}C-NMR (T 298 K): δ 190.33 (2C, $J(^{103}Rh-^{13}C)$ 85 Hz, C≡O), 117.38 (2C, $C_{4,5}$), 113.49 (2C, $J(^{103}Rh-^{13}C)$ ca. 4 Hz, $C_{3a,5a}$), 106.53 (2C, $J(^{103}Rh-^{13}C)$ ca. 2 Hz, $C_{1a,8a}$), 95.74 (2C, $J(^{103}Rh-^{13}C)$ 6 Hz, $C_{2,7}$), 78.24 (2C, $J(^{103}Rh-^{13}C)$ 3.4 Hz, $C_{3,6}$), and 74.65 (2C, $J(^{103}Rh-^{13}C)$ 3.4 Hz, $C_{1,8}$). The CO resonance has not been detected due to the very low signal-to-noise ratio.

3.15. 2,7-Dimethyl-as-indacene-diide-[Rh(COD)]$_2$

Yield, 80–90%. *Syn/anti* ratio: 2:1. *Syn* isomer: ^{1}H-NMR (CD$_2$Cl$_2$, T 298 K, ppm from internal TMS): δ 6.73 (m, 2H, H$_{4,5}$), 5.13 (m, 2H, H$_{1,8}$), 4.90 (m, 2H, H$_{3,6}$), 4.02 and 3.90 (2m, 4H each, olefin protons of COD), 2.29 (s, 6H, 2,7-CH$_3$), and 2.2–1.6 (m, 16H, methylene protons of COD). ^{13}C-NMR (T 298 K): δ 116.7 (2C, $C_{4,5}$), 107.1 (2C, $J(^{103}Rh-^{13}C)$ 2.7 Hz, $C_{2a,7a}$), 106.1 (2C, $J(^{103}Rh-^{13}C)$ 4.5 Hz, $C_{3a,5a}$), 105.4 (2C, $J(^{103}Rh-^{13}C)$ 4.5 Hz, $C_{1a,8a}$), 79.4 (2C, $J(^{103}Rh-^{13}C)$ 3.6 Hz, $C_{1,8}$), 78.6 (2C, $J(^{103}Rh-^{13}C)$ 4.5 Hz, $C_{3,6}$), 68.6 and 67.3 (4C each, $J(^{103}Rh-^{13}C)$ 14.3 and 14.4 Hz, olefin carbons of COD), 32.4 and 32.3 (4C each, methylene carbons of COD), and 14.7 (2C, 2,7-CH$_3$). *Anti* isomer: ^{1}H-NMR (CD$_2$Cl$_2$, T 298 K, ppm from internal TMS): δ 6.77 (m, 2H, H$_{4,5}$), 5.19 (m, 2H, H$_{1,8}$), 5.08 (m, 2H, H$_{3,6}$), 3.78 and 3.26 (2m, 4H each, olefin protons of COD), 2.21 (s, 6H, 2,7-CH$_3$), and 2.2–1.6 (m, 16H, methylene protons of COD). ^{13}C-NMR (T 298 K): δ 115.6 (2C, $C_{4,5}$), 107.7 (2C, $J(^{103}Rh-^{13}C)$ 2.7 Hz, $C_{2a,7a}$), 104.3 (2C, $J(^{103}Rh-^{13}C)$ 4.5 Hz, $C_{3a,5a}$), 99.5 (2C, $J(^{103}Rh-^{13}C)$ 4.5 Hz, $C_{1a,8a}$), 81.2 (2C, $J(^{103}Rh-^{13}C)$ 4.5 Hz, $C_{1,8}$), 78.6 (2C, $J(^{103}Rh-^{13}C)$ 4.5 Hz, $C_{3,6}$), 69.7 and 66.6 (4C each, $J(^{103}Rh-^{13}C)$ 14.3 and 14.4 Hz, olefin carbons of COD), 34.1 and 30.8 (4C each, methylene carbons of COD), and 14.7 (2C, 2,7-CH$_3$).

3.16. 2,7-Dimethyl-as-indacene-diide-[Rh(NBD)]$_2$

Yield, 50%. *Syn/anti* ratio: 4.5:1. *Syn* isomer: ^{1}H-NMR (CD$_2$Cl$_2$, T 298 K, ppm from internal TMS): δ 6.65 (m, 2H, H$_{4,5}$), 5.30 (m, 2H, H$_{1,8}$), 5.19 (m, 2H, H$_{3,6}$), 3.29 (m, 4H, NBD bridgehead protons), 3.27 and 3.10 (2m, 4H each, olefin protons of NBD), 2.23 (s, 6H, 2,7-CH$_3$), and 0.87 (t, 4H, methylene protons of NBD). ^{13}C-NMR (T 298 K): δ 117.13 (2C, $C_{4,5}$), 103.73 (2C, $C_{2a,7a}$), 103.23 (2C, $C_{3a,5a}$), 102.32 (2C, $C_{1a,8a}$), 78.02 (2C, $J(^{103}Rh-^{13}C)$ 4.9 Hz, $C_{3,6}$), 76.71 (2C, $J(^{103}Rh-^{13}C)$ 4.2 Hz, $C_{1,8}$), 56.21 (2C each, $J(^{103}Rh-^{13}C)$ 6.7 Hz,

methylene carbons of NBD), 47.92 (4C each, $J(^{103}Rh-^{13}C)$ 2.4 Hz, bridgehead carbons of NBD), 34.70 and 34.57 (4C each, $J(^{103}Rh-^{13}C)$ 10.5 Hz, olefin carbons of NBD), and 15.01 (2C, 2,7-CH$_3$). *Anti* isomer: ^{1}H-NMR (CD$_2$Cl$_2$, T 298 K, ppm from internal TMS): δ 6.75 (m, 2H, H$_{4,5}$), 5.29 (m, 2H, H$_{1,8}$), 5.16 (m, 2H, H$_{3,6}$), 3.14 (m, 4H, NBD bridgehead protons), 3.02 and 2.66 (2m, 4H each, olefin protons of NBD), 2.21 (s, 6H, 2,7-CH$_3$), and 0.77 (t, 4H, methylene protons of NBD). ^{13}C-NMR (T 298 K): δ 116.08 (2C, $C_{4,5}$), $C_{2a,7a}$, $C_{3a,5a}$, and $C_{1a,8a}$ not observed, 78.92 (2C, $J(^{103}Rh-^{13}C)$ 4.3 Hz, $C_{1,8}$), 75.98 (2C, $J(^{103}Rh-^{13}C)$ 4.3 Hz, $C_{3,6}$), 56.80 (2C each, $J(^{103}Rh-^{13}C)$ 6.7 Hz, methylene carbons of NBD), 47.31 (4C each, $J(^{103}Rh-^{13}C)$ 2.4 Hz, bridgehead carbons of NBD), 34.59 and 33.04 (4C each, $J(^{103}Rh-^{13}C)$ 10.5 Hz, olefin carbons of NBD), and 14.93 (2C, 2,7-CH$_3$).

3.17. 2,7-Dimethyl-as-indacene-diide-[Rh(η^2-C$_2$H$_4$)$_2$]$_2$

Yield, 40%. *Syn/anti* ratio: 2:1. *Syn* isomer: ^{1}H-NMR (CD$_2$Cl$_2$, T 298 K, ppm from internal TMS): δ 6.73 (m, 2H, H$_{4,5}$), 5.29 (m, 2H, H$_{3,5}$), 5.22 (m, 2H, H$_{1,8}$), 2.19 (s, 6H, 2,7-CH$_3$), and 2.0 (broad signal, 16H, ethylene protons). ^{13}C-NMR (T 298 K): δ 118.57 (2C, $C_{4,5}$), 104.9 (2C, $J(^{103}Rh-^{13}C)$ 3.9 Hz, $C_{2a,7a}$), 104.4 (2C, $J(^{103}Rh-^{13}C)$ 4.1 Hz, $C_{3a,5a}$), 103.0 (2C, $J(^{103}Rh-^{13}C)$ 3.7 Hz, $C_{1a,8a}$), 81.62 (2C, $J(^{103}Rh-^{13}C)$ 4.3 Hz, $C_{3,6}$), 80.90 (2C, $J(^{103}Rh-^{13}C)$ 4.1 Hz, $C_{1,8}$), 44.3 (broad signal, 8C, ethylene carbons), and 14.015 (2C, 2,7-CH$_3$). *Anti* isomer: ^{1}H-NMR (CD$_2$Cl$_2$, T 298 K, ppm from internal TMS): δ 6.84 (m, 2H, H$_{4,5}$), 5.309 (m, 2H, H$_{1,8}$), 5.17 (m, 2H, H$_{3,6}$), 2.16 (s, 6H, 2,7-CH$_3$), and 1.7 (broad signal, 16H, ethylene protons). ^{13}C-NMR (T 298 K): δ 116.69 (2C, $C_{4,5}$), 104.8 (2C, $J(^{103}Rh-^{13}C)$ 4.8 Hz, $C_{2a,7a}$), 104.2 (2C, $J(^{103}Rh-^{13}C)$ 4.3 Hz, $C_{3a,5a}$), 97.1 (2C, $J(^{103}Rh-^{13}C)$ ca. 2 Hz, $C_{1a,8a}$), 83.37 (2C, $J(^{103}Rh-^{13}C)$ 3.6 Hz, $C_{3,6}$), 79.77 (2C, $J(^{103}Rh-^{13}C)$ 4.2 Hz, $C_{1,8}$), 43.2 (broad signal, 8C ethylene carbons), and 13.82 (2C, 2,7-CH$_3$).

3.18. 2,7-Dimethyl-as-indacene-diide-[Rh(CO)$_2$]$_2$

Yield, 45%. *Syn/anti* ratio: 1:1.5. *Syn* isomer: ^{1}H-NMR (CD$_2$Cl$_2$, T 298 K, ppm from internal TMS): δ 6.97 (m, 2H, H$_{4,5}$), 6.12 (m, 2H, H$_{1,8}$), 5.52 (m, 2H, H$_{3,6}$), and 2.26 (s, 6H, 2,7-CH$_3$). *Anti* isomer: ^{1}H-NMR (CD$_2$Cl$_2$, T 298 K, ppm from internal TMS): δ 6.94 (m, 2H, H$_{4,5}$), 5.78 (m, 2H, H$_{1,8}$), 5.73 (m, 2H, H$_{3,6}$), and 2.29 (s, 6H, 2,7-CH$_3$).

3.19. 2,7-Dimethyl-as-indacene-diide-[Ir(CO)$_2$]$_2$

Yield, 45%. *Syn/anti* ratio: 1:1.5. *Syn* isomer: IR (CH$_2$Cl$_2$): ν(CO) 2042, 2026, 1974, and 1959 cm^{-1};

Table 5

Summary of crystal and intensity data for 2,7-dimethyl-*as*-indacene-diide-[Rh(COD)] (*syn*-Rh$_2$) and 2,7-dimethyl-*as*-indacene-diide-[Ir(COD)] (*syn*-Ir$_2$)

	syn-Rh$_2$	*syn*-Ir$_2$
Formula	RhC$_{15}$H$_{18}$	IrC$_{15}$H$_{18}$
Molecular weight	301.21	390.55
Space group	$P2_1/a$	$P2_1/a$
a (Å)	6.793(1)	6.828(1)
b (Å)	30.916(3)	31.248(3)
c (Å)	11.312(2)	11.360(2)
α (°)	90	90
β (°)	100.9(1)	100.6(1)
γ (°)	90	90
V (Å^3)	2332.8	2382.4
Z	4	4
Crystal dimensions (mm^3)	0.2 × 0.2 × 0.4	0.25 × 0.3 × 0.35
$D_{calc.}$ (g cm^{-3})	1.72	2.18
μ (cm^{-1})	12.91	107.6
T (K)	298	298
Radiation	Graphite-monochromated	Mo–K$_\alpha$ ($\lambda = 0.7107$ Å)
Take off angle (°)	3	3
Scan speed (deg min^{-1})	2.0 in the 2θ scan mode	2.0 in the 2θ scan mode
2θ range (°)	$3.0 \leq 2\theta \leq 45$	$3.0 \leq 2\theta \leq 45$
Observed reflections [$F_o^2 \geq 3\sigma(F_o^2)$]	2624	3598
R (on F_o)	0.067	0.064
R_w	0.063	0.060
G.O.F.	0.98	1.02

^{1}H-NMR (CD$_2$Cl$_2$, *T* 298 K, ppm from internal TMS): δ 7.14 (m, 2H, H$_{4,5}$), 6.15 (m, 2H, H$_{1,8}$), 5.51 (m, 2H, H$_{3,6}$), and 2.46 (s, 6H, 2,7-CH$_3$). *Anti* isomer: IR (CH$_2$Cl$_2$): ν(CO) 2042 and 1966 cm^{-1}; ^{1}H-NMR (CD$_2$Cl$_2$, *T* 298 K, ppm from internal TMS): δ 7.08 (m, 2H, H$_{4,5}$), 5.81 (m, 2H, H$_{1,8}$), 5.72 (m, 2H, H$_{3,6}$), and 2.50 (s, 6H, 2,7-CH$_3$).

3.20. Carbonylation of syn- and anti-{2,7-dimethyl-as-indacene-diide-[Rh(COD)]$_2$}

Pre-cooled CO was bubbled into a 2 × 10^{-2} M solution in CH$_2$Cl$_2$ of the 2:1 mixture of *syn*- and *anti*-{2,7-dimethyl-*as*-indacene-diide-[Rh(COD)]$_2$} cooled to −78°C. By using a cool syringe, at appropriate times, 5 ml portions were taken into a cool Schlenk tube (*T* ca. −100°C) and pumped to dryness at high vacuum by using a liquid-nitrogen-cooled trap. The residue was dissolved in 0.5 ml of CD$_2$Cl$_2$ and the solution analyzed by NMR for the components.

3.20.1. syn-{2,7-Dimethyl-as-indacene-diide-[η^5-Rh(CO)$_2$][η^5-Rh(COD)]} (syn-I)

^{1}H-NMR (CD$_2$Cl$_2$, *T* 298 K): δ 6.881 and 6.836 (1H each, AB quartet, J_{AB} 10 Hz, H$_5$ and H$_4$, respectively),

5.674 (m, 1H, H$_8$), 5.659 (m, 1H, H$_1$), 5.133 (m, 1H, H$_6$), 5.001 (m, 1H, H$_3$), 4.098 and 3.427 (2m, 2H each, COD olefin protons), 2.396 (s, 3H, 7-CH$_3$), 2.266 (s, 3H, 2-CH$_3$), and 1.9-1.7 (m, 8H, COD methylene protons).

3.20.2. anti-{2,7-Dimethyl-as-indacene-diide-[η^5-Rh(CO)$_2$][η^5-Rh(COD)]} (anti-I)

^{1}H-NMR (CD$_2$Cl$_2$, *T* 298 K): δ 6.902 and 6.843 (1H each, AB quartet, J_{AB} 10 Hz, H$_5$ and H$_4$, respectively), 5.723 (m, 1H, H$_8$), 5.676 (m, 1H, H$_1$), 5.200 (m, 1H, H$_6$), 5.082 (m, 1H, H$_3$), 3.919 and 3.632 (2m, 2H each, COD olefin protons), 2.373 (s, 3H, 7-CH$_3$), 2.252 (s, 3H, 2-CH$_3$), and 1.9-1.7 (m, 8H, COD methylene protons).

3.21. Carbonylation of syn- and anti-{2,7-dimethyl-as-indacene-diide-[Ir(COD)]$_2$}

Pre-cooled CO was bubbled for 1 h into a 2 × 10^{-2} M solution in CD$_2$Cl$_2$ of the 2:1 mixture of *syn*- and *anti* - {2,7 - dimethyl - *as* - indacene - diide - [Ir(COD)]$_2$} cooled to −40°C, and the solution analyzed by NMR for the components. No changes were observed for the resonances of the *anti* derivative.

3.21.1. syn-{2,7-Dimethyl-1,6-dihydro-1,6-[η^1-Ir(COD)(CO)$_2$]$_2$-as-indacene} (A)

^{1}H-NMR (CD$_2$Cl$_2$, *T* 233 K): δ 7.12 and 6.91 (2H, AB quartet, J_{AB} 9.1 Hz, H$_5$ and H$_4$, respectively), 6.33 (m, 1H, H$_8$), 6.16 (m, 1H, H$_3$), 3.6 (broad m, 1H, H$_6$), 3.1 (broad m, 1H, H$_1$), 4.04 (broad m, olefin protons of COD), 2.65 (m, methylene protons of COD), 2.29 (s, 3H, 2-CH$_3$), and 2.26 (s, 3H, 7-CH$_3$).

3.21.2. syn-{2,7-Dimethyl-3,6-dihydro-3,6-[η^1-Ir(COD)(CO)$_2$]$_2$-as-indacene} (B)

^{1}H-NMR (CD$_2$Cl$_2$, *T* 233 K): δ 7.21 (s, 2H, H$_{4,5}$), 6.33 (m, 1H, H$_8$), 6.39 (m, 2H, H$_{1,8}$), 3.6 (broad m, 2H, H$_{3,6}$), 4.04 (broad m, olefin protons of COD), 2.65 (m, methylene protons of COD), and 2.33 (s, 6H, 2- and 7-CH$_3$).

3.22. Crystal-structure determination

Suitable crystals of *syn*-Rh$_2$ and *syn*-Ir$_2$, grown from THF–hexane solutions, were mounted on a Philips PW-100 computer-controlled four-circle diffractometer with graphite monochromator (Mo–K$_\alpha$ radiation). Indexing of 25 high-angle reflections followed by short preliminary data collection led to the assignment of the monoclinic space group $P2_1/a$. The intensities were corrected for the usual geometrical factors, an empirical absorption correction was also applied (ψ scan). The initial Patterson map was solved for Rh and Ir posi-

tions; the molecules were developed by subsequent difference syntheses and least-squares refinements. Almost all the hydrogen atoms, except those of the methyl groups, were located from the final difference Fourier syntheses; yet they were geometrically recalculated and assigned isotropic temperature factors 1.2 times as large as the equivalent isotropic temperature factor of their pivot carbon atoms were included in the final calculations but not refined. The thermal parameters for all the non hydrogen atoms were treated anisotropically. The model converged to give weighted and unweighted R factors of 0.064 and 0.069 for syn-Rh_2, and 0.070 and 0.072 for syn-Ir_2, respectively. In the final difference map the largest residual peak was less than 0.50 e $Å^{-3}$, apart from the heavy atoms ripples. Crystal data and intensity data are reported in Table 5.

4. Supplementary material

The final positions as well as thermal and anisotropic parameters and a complete list of bond lengths and bond angles have been deposited with the Cambridge Crystallographic Data Centre. Copies of this information may be obtained free of charge from The Director, CCDC, 12 Union Road, Cambridge CB2 1EZ, UK (fax: +44-1223-336033; e-mail: deposit@ccdc.cam.ac.uk or www: http://www.ccdc.cam.ac.uk).

References

[1] (a) E.L. Mutterties, M.J. Krause, Angew. Chem. Intl. Ed. Engl. 22 (1983) 147. (b) D.A. Roberts, G.L. Geoffroy, in: G. Wilkinson, F.G.A. Stone, E.W. Abel (Eds.), Comprehensive Organometallic Chemistry, vol. 6, Pergamon, Oxford, 1982, pp. 763–877, Ch. 40. (c) W.L. Gladfelter, G.L. Geoffroy, Adv. Organomet. Chem. 18 (1980) 207. (d) W. Beck, B. Niemer, M. Wieser, Angew. Chem. Intl. Ed. Engl. 32 (1993) 923.

[2] (a) R.C. Kerber, B.R. Waldbaum, J. Organomet. Chem. 513 (1996) 277, and references cited therein. (b) R. Fierro, T.E. Bitterwolf, A.L. Rheingold, G.P.A. Yap, L.M. Liable-Sands, J. Organomet. Chem. 524 (1996) 19, and references cited therein. (c) I. Kovács, M.C. Baird, Organometallics 15 (1996) 3588. (d) S.S. Lee, T.-Y. Lee, J.E. Lee, I.-S. Lee, Y.K. Chung, Organometallics 15 (1996) 3664. (e) U. Behrens, H. Brussard, U. Hagenau, J. Heck, E. Hendrickx, J. Körnich, J.G.M. van der Linden, A. Parsoons, A.L. Spek, N. Veldman, B. Vos, H. Wong, Chem. Eur. J. 2 (1996) 98. (f) W. Zhang, S.R. Wilson, D.N.

Hendrickson, Inorg. Chem. 28 (1989) 4160. (g) T.E. Bitterwolf, A.L. Rheingold, Organometallics 6 (1987) 2138, and references cited therein. (h) T.E. Bitterwolf, J. Organomet. Chem. 320 (1987) 121. (i) T.E. Bitterwolf, J. Organomet. Chem. 312 (1986) 197. (j) J.C. Smart, B.L. Pinsky, J. Am. Chem. Soc. 99 (1977) 956.

[3] (a) A. Miyake, A. Kanai, Angew. Chem. Intl. Ed. Engl. 10 (1971) 801. (b) E.E. Bunel, A.L. Valle, N.L. Jones, P.J. Carroll, C. Barra, M. Gonzalea, N. Munoz, G. Visconti, A. Aizman, J.M. Manriquez, J. Am. Chem. Soc. 110 (1988) 6596.

[4] (a) K. Jonas, Pure Appl. Chem. 62 (1990) 1169. (b) B.F. Bush, V.M. Lynch, J.J. Lagowski, Organometallics 6 (1987) 1267. (c) M.A. Bennett, H. Neumann, M. Thomas, X. Wang, P. Pertici, P. Salvadori, G. Vitulli, Organometallics 10 (1991) 3237. (d) S. Sun, C.A. Dullaghan, G.B. Carpenter, A.L. Rieger, P.H. Rieger, D.A. Sweigart, Angew. Chem. Intl. Ed. Engl. 34 (1995) 2540.

[5] (a) A. Ceccon, A. Gambaro, S. Santi, G. Valle, A. Venzo, J. Chem. Soc. Chem. Commun. (1989) 52. (b) C. Bonifaci, A. Ceccon, A. Gambaro, P. Ganis, S. Santi, G. Valle, A. Venzo, Organometallics 12 (1993) 4211. (c) C. Bonifaci, A. Ceccon, A. Gambaro, P. Ganis, S. Santi, A. Venzo, Organometallics 14 (1995) 2430. (d) C. Bonifaci, A. Ceccon, A. Gambaro, P. Ganis, S. Santi, G. Valle, A. Venzo, J. Organomet. Chem. 492 (1995) 35. (e) C. Bonifaci, G. Carta, A. Ceccon, A. Gambaro, S. Santi, A. Venzo, Organometallics 15 (1996) 1630. (f) C. Bonifaci, A. Ceccon, A. Gambaro, P. Ganis, L. Mantovani, S. Santi, A. Venzo, J. Organomet. Chem. 475 (1994) 267. (g) L. Mantovani, A. Ceccon, A. Gambaro, S. Santi, P. Ganis, A. Venzo, Organometallics 16 (1997) 2682.

[6] (a) S. Barlow, D. O'Hare, Chem. Rev. 97 (1997) 637. (b) D. Astruc, Acc. Chem. Res. 30 (1997) 383. (c) M.D. Ward, Chem. Soc. Rev. 30 (1997) 12.

[7] M.T. Garland, J.-Y. Saillard, I. Chávez, B. Oëlckers, J.M. Manriquez, J. Mol. Struct. (Theochem.) 390 (1997) 199.

[8] J.M. Manriquez, M.D. Ward, W.M. Reiff, J.C. Calabrese, N.L. Jones, P.J. Carroll, E.E. Bunel, J.S. Miller, J. Am. Chem. Soc. 177 (1995) 6182 and references therein.

[9] (a) W.A. Bell, C.J. Curtis, C.W. Eigenbrot, Jr., C.G. Pierpont, J.L. Robbins, J.C. Smart, Organometallics 6 (1987) 266. (b) W.L. Bell, C.J. Curtis, A. Miedaner, C.W. Eigenbrot, Jr., R.C. Haltiwanger, C.G. Pierpont, J.C. Smart, Organometallics 7 (1988) 691.

[10] (a) P. Roussel, M.J. Drewitt, D.R. Cary, C.G. Webster, D. O'Hare, Chem. Commun. (Cambridge) (1998) 2205. (b) D.R. Cary, C.G. Webster, M.J. Drewitt, S. Barlow, J.C. Green, D. O'Hare, Chem. Commun. (Cambridge) (1997) 953. (c) D.R. Cary, J.C. Green, D. O'Hare, Angew. Chem. Int. Ed. Engl. 36 (1997) 2618.

[11] A. Bisello, A. Ceccon, A. Gambaro, P. Ganis, F. Manoli, S. Santi, A. Venzo, J. Organomet. Chem. (in press).

[12] J. Hiermeier, F.H. Köhler, G. Müller, Organometallics 10 (1991) 1787.

[13] (a) U. Englert, U. Koelle, Z. Kristallogr. 211 (1996) 64. (b) B. Denise, D. Brodzhi, G. Pannetier, Bull. Soc. Chim. Fr. 5–6 (1975) 1034. (c) J.A. Ibers, R.G. Snyder, Acta Crystallogr. 15 (1962) 923. (d) D.J.A. De Ridder, P. Imhoff, Acta Crystallogr. Sect. C 50 (1994) 1569. (e) R.A. Epstein, G.L. Geoffroy, M.E. Keeney, W.R. Mason, Inorg. Chem. 18 (1979) 478. (f) R. Cramer, Inorg. Chem. 1 (1962) 722. (g) L.F. Dahl, C. Martell, D.L. Wampler, J. Am. Chem. Soc. 83 (1961) 1761. (h) L. Walz, P. Scheer, Acta Crystallogr. Sect. C 47 (1991) 640. (i) J.G. Norman, Jr., D.J. Gmur, J. Am. Chem. Soc. 99 (1977) 1446.

[14] P. Ganis, A. Ceccon, T. Köhler, F. Manoli, S. Santi, A. Venzo, Inorg. Chem. Commun. 1 (1998) 15.

[15] (a) M.E. Rerek, F. Basolo, Organometallics 2 (1983) 372. (b) C. Moreno, M.J. Macazaga, S. Delgado, Organometallics 10 (1991) 1124. (c) M. Cheong, F. Basolo, Organometallics 7 (1988) 2041. (d) M.E. Rerek, F. Basolo, J. Am. Chem. Soc. 106 (1984) 5908. (e) A.K. Kakkar, N.J. Taylor, T.B. Marder, J.K. Shen, N. Hallinan, F. Basolo, Inorg. Chim. Acta 198–200 (1992) 219.

[16] S. Bellomo, A. Ceccon, A. Gambaro, S. Santi, A. Venzo, J. Organomet. Chem. 453 (1993) C4.

[17] A. Venzo, A. Bisello, A. Ceccon, F. Manoli, S. Santi, Inorg. Chem. Commun. (in press).

[18] A. Bax, S. Subramanian, J. Magn. Reson. 67 (1986) 565.

[19] (a) G. Otting, K. Wüthrich, Magn. Reson. 76 (1988) 569. (b) G. Drobny, A. Pines, S. Sinton, D. Weitekamp, D. Wemmer, Faraday Symp. Chem. Soc. 13 (1979) 49.

[20] A. Bax, M.F. Summers, J. Am. Chem. Soc. 108 (1986) 2093.

[21] L. Trogen, U. Edlund, Acta Chem. Scand. B 33 (1979) 109.